Title

THE LOW-TEMPERATURE HEAT CAPACITY OF CERIUM METAL

Author

Conway, Mary Macivor.

Publication Date

1972-05-01

Thesis/dissertation

LBL-827

THE LOW-TEMPERATURE HEAT CAPACITY OF CERIUM METAL

Mary MacIvor Conway
(Ph. D. Thesis)

May 1972

AEC Contract No. W-7405-eng-48

LBL-827

DISCLAIMER

Outline

THE LOW-TEMPERATURE HEAT CAPACITY OF CERIUM METAL

Mary MacIvor Conway

Inorganic Materials Research Division, Lawrence Berkeley Laboratory
and Department of Chemistry; University of California,
Berkeley, California

ABSTRACT

The heat capacities of mixtures of the α and β phases of Ce metal were measured between 0.08 and 24 K at zero pressure and in zero field. Two were also measured between 0.4 and 24 K in fields of up to 60.5 kOe. The heat capacities of the pure phases were extrapolated from this data. α Ce has a γ of 22 $mJ/mole \cdot K^2$, showing the expected large f contribution, and a θ of 125 K. The low temperature heat capacity of β Ce is field independent to 60.5 kOe. It can be represented by a linear term with $\gamma = 54$ $mJ/mole \cdot K^2$ and a T^3 term an order of magnitude larger than that expected from the lattice contribution. Existing theories seem inadequate to explain the large size of the former and the field independence of the latter. The entropy associated with the 12.5 K ordering peak shows it to involve only half the sites of the dhcp β phase.

INTRODUCTION

Properties of Cerium

The variable valence of the element Ce has been a major factor in the continuing interest and research into its properties. The 4f, 5d, and 6s levels are of comparable energy in the Ce free atom and retain similar energies in Ce metal.[1,2] Their exact relationship is affected by pressure and temperature, with high pressures and low temperatures raising the energy of the 4f level with respect to the Fermi level of the s-d conduction band.[3-5] The 4f level has a radius of only 1/10 the atomic radius, and is inside and well shielded by the filled 5s and 5p shells, so that the behavior of the one 4f electron should be free atom-like in trivalent Ce[1,6] where the energy of the 4f level is well below the Fermi level. When its energy is well above the Fermi level, its electron will be transferred to the conduction band, changing the Ce to tetravalent. At least most and possibly all of this change in valence can be made continuously in Ce, but large discontinuous changes in valence do occur at some phase boundaries. The statements are not contradictory; metallic Ce has at least one critical point, as shown in the phase diagram in Figure 1. The phase boundaries shown are the estimated thermodynamic boundaries, based on 3 sets of measurements which cover the known transitions.[7-9] The positions of the boundaries may be shifted by impurities,[10] and are usually obscured by hysteresis (as large as 190 K[7] or 43 kbar[11]), so that discrepancies do exist in reported values, but the discrepancies are not important here.

The three low pressure, high temperature phases of Ce appear to have very similar valences, near 3.06. No purely trivalent phase is known. The three phases are the body-centered cubic (bcc) δ phase stable between 1000 and 1070 K at one atmosphere, the face-centered cubic (fcc) γ phase stable between 350 and 1000 K, and the double hexagonal close-packed (dhcp) β phase stable between 140 and 350 K. In the case of the little studied δ phase, this estimate of the valence is based on the similarity of its molar volume and that of γ Ce.[8] The β and γ phases have a 4f electron which generally acts well localized. The metastable β phase orders antiferromagnetically at 12.5 K.[12] (The γ phase is not present at such low temperatures in sufficient quantities for its expected ordering to be detectable.) The magnetic susceptibilities of both the β and γ phases obey a Curie-Weiss law above 110 K, with an effective atomic moment of 2.51 μ_B, close to the free atomic value of 2.54 μ_B.[6] This implies a valence of approximately 3.03.[13] The observed metallic radii of 1.824 for γ Ce and 1.826 for β Ce are smaller than the value of 1.846 estimated for trivalent Ce (at room temperature and 1 atmosphere) from the observed values of the radii of the other trivalent rare earths.[13] Either the variation of the metallic radii along the rows of the periodic table[13] or the observed radius of α Ce[14] may be used to estimate the radius of tetravalent Ce. Both indicate a valence of 3.11 to 3.13 for β and γ Ce.

This valence is not constant with temperature and pressure in γ Ce and is probably not constant in β Ce. The γ phase has a higher valence near the γ-α phase boundary than it does at room temperature

and 1 atmosphere. Elastic constant measurements at 1 atmosphere show a lattice softening in a mixture of β Ce and metastable γ Ce between 175 K and the γ → α transition at 110 K, which continues to 31 K in the mixture of α Ce and metastable β Ce.[15] (This metastable γ ⇌ α phase boundary lies slightly above the β ⇌ α boundary near 140 K and also has a large hysteresis.) This behavior is apparently associated with an increase in the valence of the β and γ phases. It is also observed in samples containing only the γ phase.[16] At room temperature, the compressibility of γ Ce increases with pressure[17,18] while its susceptibility decreases.[19] Both indicate an increase in valence before the γ → α transition near 7 kbar. Both γ and α Ce have the same valence above their critical point (α Ce is also fcc), but the γ phase changes its lattice constant and presumably its valence much less than does the α during the approach to the critical point.[17]

The low temperature γ → α transition at 1 atmosphere is associated with a 17% decrease in volume[7] and with large changes in the susceptibility,[6] resistivity,[20] and Hall effect[21] of the sample. The high pressure, room temperature transition shows a 12% volume change,[7] evidence that one or both of the phases has changed its valence during the increase in pressure and temperature. Changes in the susceptibility[19] and resistivity[11] are also observed at the room temperature transition. The susceptibility change appears to be twice as large as the change at the low temperature transition,[22] but the presence of an uncertain amount of β phase makes the comparison very approximate. The atomic volume and susceptibility data indicate a valence of 3.55 to 3.76

for α Ce at low temperatures and 1 atmosphere and one of 3.49 to 3.74 for α Ce at room temperature and 7 to 10 kbar.[13,19]

The valence of α Ce is not constant. At room temperature and high pressure, it has a higher compressibility near the γ-α transition than it has at higher pressures.[18] The change in lattice constant along the phase boundary approaching the critical point is mostly in the α phase[17] and is faster above 500 K than below.[17,18] The susceptibility of α Ce shows a linear decrease as pressure increases up to 18 kbar at room temperature,[19] but its lattice constant[14] and resistivity[11] decrease more rapidly at lower pressures than at pressures above approximately 25 kbar. All indicate an increase in valence as the pressures increases. There is no region of more rapid valence change near the α-α' transition,[11,14] in contrast to the behavior near the γ-α transition, and the volume change is only 4.37%.[14] Assuming the α' phase to be fully tetravalent, and comparing the 4.37% volume change at the 50 kbar transition with the 34.52% volume change necessary to go from the hypothetical tetravalent state to the trivalent state at room temperature,[13] this implies α Ce has a valence of 3.87 at 50 kbar and room temperature.

A few other properties of α Ce should be mentioned here. Though they do not lend themselves to valence computations, they must be accounted for by any theoretical models of the band structure responsible for non-integral valences. No magnetic ordering transition has been detected in α Ce.[12,19] Neutron diffraction measurements indicate that α Ce has no uncompensated spins at zero pressure[12] but may not

be conclusive evidence for that point.[13] The susceptibility of α Ce at 10 kbar is temperature independent above 100 K, behavior typical of a metal with no localized magnetic moment. It is unusually large, showing a large exchange enhancement apparently associated with localized electrons.[19] Finally, it increases in value below 100 K, atypical behavior whose origin is uncertain.[19] No superconducting transition has been detected in α Ce above 0.3 K at 10 kbar[23,24] or above 1.3 K at 50 kbar.[11] Localized moments inhibit superconductivity or surpress it entirely,[3-5] but are not the only possible reason for the failure to detect superconductivity. The IVb elements Ti, Zr, and Hf have their transitions at 0.44, 0.56, and 0.16 respectively,[25] and the IIIb elements Sc and Y are not superconducting at zero pressure,[26,27] though none of these elements is magnetic. The virtual bound state model of the 4f level in Ce,[28,29] which appears to be the model best able to describe the observed properties of Ce, predicts that α Ce is superconducting but at temperatures just below those investigated.

The α' phase of Ce appears fully tetravalent. It undergoes no compression between 50 and 82.5 kbar.[14] It is superconducting, with a transition temperature of 1.7 K at 50 kbar which follows the common pattern of decreasing as pressure increases.[11] Its lattice structure and certain aspects of its phase boundary are controversial. It has been reported as both fcc[14] and distorted hexagonal close-packed (hcp).[30] Jayaraman's failure to find any evidence that an α-α' boundary intersects the fusion curve[8] supports the fcc structure in that it suggests

that the boundary ends in a critical point. No direct evidence for a critical point was obtained in the measurement of the boundary, which unfortunately do not go above 480 K. The change in resistance across the boundary is approximately constant, and the valences of the α and α' phases do not change rapidly on each side of the transition. The question of lattice structure is important, since the virtual bound state model predicts a continuous change to tetravalency in α Ce.[28,29] A first order transition to an fcc α' phase implies a fundamental change in electronic properties not predicted by the model. A transition to an hcp (or other non-fcc) α' phase does not rule out a continuous change to tetravalency in metastable α Ce at pressures above 50 kbar.

Studies of Ce at 2 different valences are possible at low temperatures because the α phase is stable and the β phase metastable to zero K at zero pressure. They are also difficult, since in this region samples of Ce almost inevitably contain both phases in uncertain amounts. Because of the large hysteresis associated with the phase transitions of Ce, a sample of Ce freshly cooled from the melt or from a high temperature anneal will generally remain entirely in the γ phase at room temperature. When it is first cooled below approximately 280 to 250 K, some 30 to 80% of the sample transforms to the β phase, while the remaining 20 to 70% remains in the γ phase until approximately 100 to 30 K, where it transforms to the α phase. Little if any γ phase is retained at zero K. Some β phase converts to α at approximately 40 to 80 K. The sample at 4.2 K will be approximately 30 to 60% β, 0 to 5% γ, and 35 to 70% α. The exact phase composition has a complex

dependence on the purity of the sample, its grain size, whether it was cold worked, how fast it was cooled, and possibly other factors. When the sample is re-warmed, the α phase reverts primarily to γ but the β phase does not revert unless the sample is warmed above approximately 350 to 440 K. Further thermal cycling increases the amount of β phase in the sample to a limiting value of approximately 60 to 90%.[7,12,31,32] So far, pure β Ce has not been obtained at 4.2K. Pure α Ce is obtainable by applying approximately 10 kbar to a pure γ sample at room temperature to convert it to pure α, and then cooling the sample under pressure to keep it outside the region of β stability.[23]

Theoretical Background

In mixed phase samples of Ce, the total heat capacity, C, is equal to the sum of the contributions from the heat capacity of the pure α and pure β phases, C_α and C_β. Small secondary contributions from other phases or from impurities may also occur. Both C_α and C_β may be further divided into components. Both have an electronic heat capacity, C_E, and a lattice heat capacity, C_L. The magnetic β Ce also has a crystal field heat capacity, C_C, and a magnetic heat capacity, C_M.

Electronic Contribution

The band structure density of electronic states at the Fermi surface, $N(\epsilon_F)$, is the major controlling factor of the magnitude of C_E. Their relationship is described by:

$$C_{Ebs} = (\pi^2 k_B^2/3)\, N(\epsilon_F) T \equiv \gamma_{bs} T \qquad (1)$$

where C_{Ebs} is the unenhanced band structure electronic heat capacity, and γ_{bs} is a temperature-independent constant. The magnitude of $N(\epsilon_F)$ is not simply dependent upon the number of conduction electrons in the metal. It strongly reflects the width of the conduction band. A broad band, such as the typical s-d conduction band, will have a low to moderate density of states over a wide range of energies, so the value of $N(\epsilon_F)$ will not be sensitive to the value of the Fermi energy, ϵ_F. A narrow band, such as the 4f band, will have a very high density of states but only in a narrow energy range, outside of which the

density of states drops rapidly to a negligible value.[1,2,28,29] If the 4f band overlaps the Fermi surface, $N(\epsilon_F)$ will be very sensitive to the position of this band relative to ϵ_F. The magnitude of $N(\epsilon_F)$ is also dependent upon the degree to which the available Fermi surface is reduced by energy gaps introduced at Brillouin zone boundaries. In general, metals with even valences undergo a greater reduction of their effective Fermi surface than do metals with odd valences.

Electron-phonon and (in magnetic materials) electron-magnon interactions can raise the effective mass of the electrons, which in turn will make C_E larger than C_{Ebs}. Theoretical studies of the magnitude and temperature dependence of these interaction effects have been done,[33-39] but there is not yet much experimental confirmation of the theories, which leaves room for considerable doubt as to how these effects should be included in the analysis of experimental data. When Equation 1 is adjusted for these effects according to the theories, the result is:

$$C_E = [1 + \lambda_p(T) + \lambda_m(T)]\, \gamma_{bs}\, T \qquad (2)$$

where λ_p is the temperature dependent parameter describing the electron-phonon enhancement effect and λ_m, also temperature dependent, describes the electron-magnon enhancement. This λ_m is zero for metals with no or with dilute localized spins,[34] and so is presumably zero for α Ce in spite of its virtual bound f level. At T = 0, where λ_p has a value of approximately 0.3 to 1.6[39] and λ_m has a value usually near 1,[34] $[1 + \lambda_p(T=0)$ and $\lambda_m(T=0)]\, \gamma_{bs} \equiv \gamma_o$. Both λ_p and λ_m are believed to

increase with T at temperatures immediately above zero, so that C_E is not a perfectly linear function of T. However, it is nearly linear at temperatures near zero, and in most cases a linear approximation is the best available for extrapolating γ_o. After this initial increase, both λ_p and λ_m pass through a maximum, which in the case of Ce is expected to be near 10 to 20 K for λ_p and near 0.2 to 1 K for λ_m. This is based in the case of λ_p on comparisons with the calculated behavior of elements with a similar Debye θ,[37,38] since λ_p depends primarily on the phonon frequencies and not on the electronic properties of the metal.[39] In the case of λ_m is is based on the assumption that the important difference between Ce and Gd, for which λ_m has been calculated,[33] is the lower magnetic exchange energy of Ce. This is not necessarily the case, since the 4f electron of β Ce may be in a magnetic virtual bound state[28,29] and much closer in energy to the Fermi level than are the 4f electrons of Gd. Above their maxima, λ_p and λ_m decay slowly to zero, so that by 150 to 200 K, C_E should be equal to C_{Ebs}. The effect of an external magnetic field on λ_m is not known.

Lattice Contribution

The Debye theory for C_L describes its behavior in terms of a constant, θ, and a universal function in temperature. In the limit of low temperature, the function takes the form $C_L = 234\ RT^3/\theta^3$, where R is the gas constant. This T^3 behavior depends only on the proportionality of the frequency spectrum to the square of the frequency at low frequencies, and must be correct at sufficiently low temperatures,

usually below $\theta/100$. Above this, the differences between the actual lattice frequency spectrum and the parabolic spectrum assumed in the Debye theory become significant. If the experimental data is fit by letting θ vary with temperature, it generally shows a minimum near θ 10, as for example in La where θ_o = 143 K, but at the minimum near 13 K, θ = 122 K.[40]

Crystal Field Contribution

The localized 4f electron in β Ce is affected by the electric fields of the neighboring atoms. When the ions are assumed to have spherical symmetry, this partially lifts the degeneracy of the $^2F_{5/2}$ ground level of the Ce^{+3} ion. The resulting levels will have degeneracies of 2 or higher, with the degeneracy and the energy separation of the levels determined by the symmetry and strength of the electric fields. In the dhcp stacking of β Ce, layers of atoms in a cubic environment alternate with layers in a hexagonal environment, so that β Ce as a whole has half of its atoms in each. For each environment separate calculations must be made of the energy levels and of the heat capacity arising from the transitions of the 4f electron between these levels. This heat capacity is of the standard Schottky form:[41]

$$C_{C_i} = \frac{R}{2ZT^2}\left\{\sum_{r=0}^{n} \epsilon_r^{\,2}\, g_r\, e^{-\epsilon_r/T} - \frac{\left[\sum_{r=0}^{n} \epsilon_r\, g_r\, e^{-\epsilon_r/T}\right]^2}{Z}\right\} \quad (3)$$

where $Z = \sum_{r=0}^{n} g_r\, e^{-\epsilon_r/T}$, ϵ_r = the energy of level r in units of K, g_r = the degeneracy of level r, R = the gas constant, and the factor of 2 adjusts for the fact that each environment i contains only half the 4f electrons.

Bleaney[42] has calculated from crystal field theory the degeneracy of the energy levels and the ratios of their splittings for both of the symmetries in α Ce, and has estimated the absolute magnitudes of the splittings by fitting his calculated C_C to the PSS[43] experimental data. He obtains 3 doublets for the hexagonal sites, at energies of zero, 30, and 150 K, and for the cubic sites a doublet at zero K and a quartet at 270 K. With these values of g_r and ϵ_r, the C_{C_i} are small below approximately 3 K, and should not interfere with the determination of γ_o, though C_{C_i} may be affected by magnetic exchange fields and deviate from the calculated curve at low temperatures.

When the effects of non-spherical symmetry in the ions are calculated, the electric quadrupole-quadrupole interaction is found to be the most important.[44] This interaction can lift the ground level degeneracy predicted on the basis of conventional crystal field effect calculations.[42] In β Ce, it could affect the atoms in the hexagonal environment, but not those in the cubic environment.[45,46] Its magnitude is estimated at 10 K for the heavier rare earths such as Gd,[44] and will be larger in the lighter rare earths where the spatial extent of the 4f electrons is greater.[44,46,1] This puts it at a magnitude comparable to that of the magnetic exchange interaction.[42] Unless the magnetic exchange is much greater than the quadrupole splitting the atoms in the hexagonal sites will have a singlet ground state. The heat capacity associated with the quadrupole splitting cannot be calculated by correcting the g_r's and ϵ_r's of equation 3, since the effect is partially co-operative in nature.[46] Theoretical calculations conflict with

experimental results,[46] so that the heat capacity contribution of a given quadrupole splitting is not really known. Experimental results on a system (Ce ethylsulphate) with a significant quadrupole splitting show a peak in the heat capacity in the same temperature range as the Schottky heat capacity (calculated ignoring the quadrupole effect), but the peak is higher and contains more entropy than the calculated Schottky.[47] Apparently the extra entropy is associated with the lifting of the degeneracy of the ground level.

Magnetic Contribution

Theory indicates that at low temperatures, the dependence of C_M on T is such that it should not interfere with the determination of γ_o. Simple spin wave theory gives $C_M \propto T^3$ for antiferromagnets. Magnetic anisotropy introduces an energy gap, Δ, into the spin wave spectrum,[48,49] leading to an exponential term in the temperature dependence of C_M. The magnitude of Δ is not known for β Ce, but the neighboring element Pr is known to have a large anisotropy.[50]

More detailed calculations of C_M from theory, and in particular quantitative comparisons with theory of the observed shape of the magnetic ordering peak in β Ce, have not been attempted primarily because of the lack of any generally accepted theory of co-operative transitions. Additionally, the inevitable strains in a multiphase sample of Ce will broaden any magnetic transition. Calculations of the entropy of ordering are both possible and useful. In such calculations it must be remembered that the 2 sites of different symmetry in β Ce

should be capable of ordering separately, as do the 2 sites in the neighboring dhcp rare earths Pr[50] and Nd.[40] When a symmetry site orders, the associated entropy will equal 1/2 R ln g_o, where g_o is the degeneracy of the ground level. In the special case of a singlet ground level, the site will not order at all unless the ratio of the exchange field to the crystal field exceeds a critical value, which in the case of a system with only a singlet excited state corresponds to an ordering temperature, T_c, of 1/10th the crystal field splitting.[51] If the system orders with T_c below the crystal field Schottky temperature, the narrow spike in the heat capacity at T_c will contain an entropy of appreciably less than 1/2 R ln 2, while the Schottky peak is broadened but not shifted in temperature.[51] The theory has not been extended to systems where T_c is comparable to the Schottky temperature. The hexagonal sites of polycrystalline Pr are such a system; no ordering peak is visible in the heat capacity of Pr. Also, the theory may not be applicable without modification to a system such as is postulated for the hexagonal sites of β Ce, where there is quadrupole rather than crystal field splitting between the 2 lowest energy states.

Secondary Contributions

There are 4 detectable secondary contributions to the heat capacity of Ce in the 0.08 to 24 K range. They appear attributable to the impurities in the cerium, to the oxidation of the sample surface, or to small amounts of a third and possibly a fourth phase of Ce. These secondary contributions are the nuclear hyperfine heat capacity, and

the small anomalies at 0.15, 0.9, and 6 K. (None of the anomalies can be ascribed to the temperature dependence of λ_m since none have a size strictly dependent on χ_β.)

The nuclear hyperfine heat capacity, C_N, is caused by the interaction between nuclear spins and ordered electron spins, and is a Schottky anomaly. Since the stable isotopes of Ce all have even-even nuclei with zero spin, Ce has no intrinsic C_N. Impurities with non-zero nuclear spins give a C_N contribution dependent on the concentration of the impurities, on the size of their nuclear spins, and on the χ_β of the sample. Since only the high temperature side of the Schottky is visible in the experimental data, the approximation $C_N \propto 1/T^2$ can be used.

The coat of Ce_2O_3 which forms on the surface of any Ce sample exposed to the air is expected to order magnetically at some temperature, since the Ce in it has a localized 4f electron.

Impurities in the bulk of a Ce sample can participate directly in an ordering transition only if they are sufficiently concentrated to order alone or as part of a Ce alloy. Such a concentration could occur with the precipitation of the impurities along grain boundaries during an annealing or a slow cooling from the melt. It should not occur when the Ce sample is quenched from the melt. Impurities may indirectly cause an ordering transition when more uniformly distributed in the sample if they stabilize otherwise unstable trivalent (and thus magnetic) phases of Ce.

EXPERIMENTAL TECHNIQUES

Heat Capacity Measurements, 0.4 - 24 K

Cryostat

The cryostat used for measurements in the 0.4 to 24 K range is not greatly different from the ones described by Triplett[52] and Senozan.[53] The chief differences are that the dewars for the cryostat are made of stainless steel and not of glass, and that a small chamber of He^4 rather than the entire He^4 bath is pumped to pre-cool the He^3 and the calorimeter to about 1.3 K before the He^3 is pumped to cool the calorimeter to 0.3 K. Stainless steel dewars are not as easily damaged as glass and can more readily be made with a large inner diameter to take a large superconducting magnet, such as was used in the course of the experiments reported here. Their disadvantage lies in their higher heat capacity and thermal conductivity, so that more liquid He^4 is required to cool stainless steel dewars and to keep them cold. Some savings on the amount of liquid He^4 needed for an experiment can be achieved by leaving the He^4 bath at one atmosphere.

The sample in its calorimeter is mounted on a brass cage anchored to the He^3 stage, as in the other cryostats, and thermal contact between the calorimeter and the He^3 stage is made and broken by means of a mechanical heat switch. The He^4 chamber cools the He^3 stage by the thermal conduction and convection of the He^3 gas in the stainless steel pumping line of the He^3 chamber (the pumping line is anchored to the He^4 chamber $3\frac{1}{2}$ in. above the top of the He^3 chamber) and by thermal conduction

along a graphite strut. This contact is adequate to cool the He^3 stage to 1.3 K as the He^4 chamber is pumped on, and it drops off sufficiently with temperature and with the reduction of the gas pressure in the He^3 pumping line that the heat leak from the He^4 chamber becomes low enough to allow the He^3 chamber to reach 0.3 K.

The superconducting magnet and its power supply were purchased from Magnion.[54] The magnet is located in the 4.2 K He^4 bath and fits over the bottom of the vacuum jacket of the cryostat, with the sample at its center. When not in use, it and its leads are taken off the cryostat to conserve liquid He^4. Similarly, when in use, current is run through the leads only during the charging and discharging of the magnet, and a persistent mode switch maintains the current for most of the time the magnet is in use. Currents of 14 and 90 Å were used, giving magnetic fields of 9.4 and 60.5 kOe, respectively. The fields were applied while the sample was at 1 to 4.2 K. The magnet gives a field on the sample which is uniform to within 0.1%. The fringe field on the Ge thermometer is merely 130 Oe when the field on the sample is 60.5 kOe. This 130 Oe is far too small to visibly affect the calibration of the thermometer.

Calorimeter

The calorimeter design shown in Figure 2 was used for all heat capacity measurements in the 0.4 to 24 K temperature range. OFHC Cu thermally links the elements necessary for a heat capacity measurement: the heater used to put heat pulses into the sample, the thermometer used to measure the resulting temperature rise and to monitor the temperature

drift between heat pulses, the sample itself, and the thermal link to the mechanical heat switch which makes or breaks thermal contact between the calorimeter and the cryostat.

The heater consists of approximately 16 feet of 0.0009 in. Pt - 9% w alloy wire wound non-inductively around a Cu post and anchored by Stycast.[55] It has a resistance of about 7,300 ohms. The 2 current and 2 voltage leads which connect the measuring circuits at room temperature with the heater are thermally anchored to each temperature stage of the cryostat to reduce the heat flow along them. The final link from the He^3 stage to the heater itself is provided by 3 identical lengths of 0.0025 in. Pt - 9% w alloy wire, which provide electrical contact while minimizing thermal contact. Only 3 of these leads are used so that the resistance measured is actually that of the heater plus that of one of the leads. This gives an automatic correction for the heat input into the calorimeter from the resistance heating in the two current-carrying leads, based on the assumption that half of this heat flows into the calorimeter and half into the cryostat.[56]

The thermometer is a Ge resistance thermometer, number 782, purchased from CryoCal[57] and calibrated in this laboratory. A Ge thermometer is used primarily because of the stability of its calibration through repeated thermal cycling. The thermal contact to the temperature sensing element of the thermometer is almost exclusively through the leads since the exchange gas in the thermometer case is deliberately chosen to be one which will be completely frozen out by 24 K, so that no anomaly in the heat capacity of the thermometer can arise when that exchange gas

condenses or freezes. The leads are thermally anchored by soldering them to Cu leads wrapped around the calorimeter and anchored to it by Stycast. The electrical connection between the thermometer and the room temperature electronics is made in much the same way as for the heater, with the exception that the link from the He^3 stage to the thermometer is made by 4 lengths of 0.003 in. manganin wire. The thermometer itself sits in a well in the Cu with its case kept in thermal contact with the well by means of a small amount of Apizon T grease.[58]

The contraction undergone by Ce metal when it passes the transition temperature to the α phase near 110 K and the rapid oxidation of Ce in air both cause problems in calorimeter design. The first was met by screwing the samples onto threaded posts so that any contraction would only increase the thermal contact between the sample and the calorimeter. The second was met by covering the sample thoroughly with a thin layer of Apiezon T grease and closely surrounding it with a Cu cup to retard the diffusion of oxygen to the surface of the cerium during the period between the final polishing of the Ce and the evacuating of the vacuum jacket around the calorimeter, a period of up to 1 hour. This arrangement does not totally prevent surface oxidation but does keep it down to a thin layer. (Experience has shown that the grease alone is sufficient for this purpose.)

Since the heat capacity of the calorimeter cannot be measured without a sample in it, a dummy sample of 16.1 g of pure Cu (99.999% pure Cominco[59] Cu melted under vacuum to remove dissolved H_2) was used

in calibrating the calorimeter. The dummy contributed slightly less than 30% of the total heat capacity. The heat capacity of the calorimeter was then determined by subtracting the heat capacity of the Cu as determined by Triplett[52] from the total, and was fit to an 8 term polynomial equation. The data points show a less then 0.2% systematic deviation from this equation, which was used to calculate the contribution of the calorimeter to the addendum. When the heater broke after being repeatedly dipped into liquid N_2 (the thermometer was protected from such abrupt temperature changes), it was re-made to the same design and the calorimeter was re-calibrated in the same manner. When the thermometer was temporarily removed from the calorimeter for further calibration, and then replaced, the amount of change which could have been caused in the heat capacity of the calorimeter was estimated to be 0.3%, so no re-calibration was done.

The calorimeter used in the Ce measurements was not calibrated in any magnetic field, but 2 calorimeters of similar construction which could be calibrated without a dummy sample had already been calibrated in zero and 60.5 kOe fields. The only field effect observed was a $1/T^2$ term in the heat capacity of the Cu, whose magnitude was consistent with that reported by Triplett[52] (the Cu of the calorimeter is not in a uniform field). Accordingly, the addenda used for the heat capacity measurements on Ce in 9.4 and 60.5 kOe fields were the zero field addendum plus a $1/T^2$ term whose magnitude was calculated from that observed in the other 2 calorimeters, with an adjustment for the small differences in the total amounts of Cu in each, and (for the 9.4 kOe

field) with an adjustment for the dependence of its size on the square of the magnetic field.

The heat capacity of the Apiezon T grease applied to the Ce samples was calculated from the smoothed data reported by Westrum et al.[60] between 1 and 25 K. Their results were extrapolated to give an additional "data point" at 0.5 K so that the low temperature end of the fit would not blow up, and then an 8 term least squares fit was used to represent the data. The fit is good to within 0.5%. The total addendum, calorimeter plus grease, was never more than 5% of the heat capacity of the Ce sample.

During the calibration of the calorimeter with the dummy Cu sample in place, the thermal relaxation times of the whole ranged from instantaneous near 0.4 K to a maximum of 50 sec at 24 K, their increase in length following the increase in total heat capacity. During the relaxation period, the temperature registered on the thermometer increased monotonically, that is, the source of the finite relaxation time was the finite time needed for the heat to travel from the heater through the sample to the thermometer, warming everything on its way. With samples in place, thermal relaxations became more complex. Superimposed on the effect just mentioned was another effect apparently associated with the 12.5 K magnetic transition in β Ce. At temperatures within a few degrees of 12.5 K, the thermometer registered a maximum temperature shortly after heat input ceased, and then showed a cooling to equilibrium. Since the calorimeter is so designed that the heat has to pass through the sample before it can reach the thermometer, the implication is that

the Ce has some slow internal relaxation in this temperature region. In the LU and RC samples the thermal relaxation times are less than 5 sec near 0.4 K and increase to less than 80 sec near 12.5 and 24 K. In the UMA and UMB samples the relaxation times are much longer at all temperatures, though their variation with temperature is the same as that observed in the LU and RC samples. For UMA, the relaxation times are about 100 sec near 0.4 K and increase to about 300 sec near 12.5 and 24 K, while for UMB the relaxation times are about 240 sec near 0.4 K and increase to about 900 sec near 12.5 and 24 K. The cause of this large difference in behavior is not clear. Because of the extrapolations necessary to correct for steady-state temperature drifts, the heat capacities of the latter two samples are not as accurate as those of the former two.

Heat Capacity Measurements, 0.08 - 0.8 K

Measurements on three samples between 0.08 and 0.8 K were made in the adiabatic demagnetization cryostat used by Triplett, and in the calorimeter designed and calibrated by him,[52] so their description will not be repeated here in any detail. The calorimeter is similar to the one used in the 0.4 to 24 K range except that it is constructed of silver, is in one piece with only one threaded post and no cup around the sample, and has a Pb superconducting switch rather than a mechanical heat switch. The Ge thermometer, number 1751, is now calibrated on the same temperature scale as thermometer 782, an improvement of the scale used by Triplett. The heat capacity of the calorimeter has been recalculated on the newer scale. The changes are not large.

The contribution of the Apiezon T grease used on the samples was corrected for as described above. Also, for the high percent β LU sample, an OFHC Cu cup with a threaded post in its center was put on the sample. This cup was weighed and its contribution to the addendum calculated from the Triplett[52] equation for Cu.

Thermal relaxation times in these low temperature experiments were 40 sec or less.

Thermometry

Temperature Scales

Recently, the National Bureau of Standards (U.S.) has announced a provisional temperature scale, T_{65},[61] for the 2 to 20 K region. This scale is based primarily on measurements of the velocity of sound in He gas and is stored on Ge resistance thermometers. Thermometers calibrated on T_{65} can be purchased from NBS. As this or perhaps some future revised scale becomes widely accepted, the extensive efforts described below will no longer be necessary for the establishment of a laboratory temperature scale, except for the continued need for magnetic thermometry to extend the scale below its present lower limit of 2 K. Meanwhile, T_{58},[62] a He^4 vapor pressure scale, is the one in common use between 1 and 4.2 K. The experimental results in this thesis are reported on the basis of T_η, a laboratory temperature scale which is based on magnetic thermometry below 1.1 K, T_{58} from 1.1 to 4.2 K, gas thermometry from 4.2 to 20 K, and the NBS platinum thermometer scale T_{55} from 15 to 25 K. Recalculation of the data on T_{65} would not alter the conclusions in this paper significantly. (The most noticeable effect would be an 0.26% increase in all electronic heat capacities.)

Calibrators

The experiments which established T_η were done in two calibrators of similar design. Both are essentially large blocks of Cu to which the various thermometers are thermally anchored. The Ge thermometers which preserve the temperature scale and the Pt thermometer calibrated

by NBS on T_{55} are mounted directly on the block. The two-bulb gas thermometer[63] is located in the block. The vapor pressure bulb used for measuring both He^4 and He^3 vapor pressures is linked to the block by lengths of Cu braid, with screw contacts at both ends (below 2.2 K, the He^4 λ point, He^4 exchange gas is used as the thermal link in vapor pressure measurements). Finally, the spherical $Ce_2Mg_3(NO_3)_{12}\cdot 24\ H_2O$ (CMN) salt pill, cut from single crystals of the salt, is varnished to two Cu vanes attached to the block with a screw contact.

Vapor Pressure Thermometry

Vapor pressure measurements were made on He^4 from 1.2 to 4.2 K, and on He^3 from 1.2 to 2.1 K (T_{62},[64] the He^3 vapor pressure scale, was defined to be consistent with T_{58}). Above the λ point, where thermal relaxation times in the He^4 bath are poor and thermal gradients exist, a small amount of liquid He^4 was condensed into the vapor pressure bulb. This bulb has Cu vanes in it to aid thermal contact and equilibrium. The tube to room temperature is vacuum jacketed to prevent the development of cold spots above the liquid, and is elaborately radiation trapped to avoid heating from radiation and from oscillations of the gas in the tube. Below the λ point, where film flow in superfluid He^4 can lead to evaporation from points at a higher temperature and make vapor pressure measurements done in an enclosed bulb suspect, the vapor pressure of the He^4 bath was measured through a tube with an open end near but always above the bath. The bath below the λ point has, of course, such a very rapid thermal equilibrium time that thermal gradients are no

longer a problem. A small amount of He^3 was condensed into the vapor pressure bulb and the vapor pressure of He^3 (which is not a superfluid) was measured at the same time. The bulb was held under vacuum at room temperature for several days between its use for measurements on He^4 and on He^3, to prevent contamination of the He^3. In spite of the change in measuring technique at the λ point, the temperature scale was smooth through this region.

During the vapor pressure measurements, pressures were measured with Hg and oil manometers, and monitored with Texas Instrument pressure gages.[65] The readings on the TI gages were displayed on a chart recorder so that any pressure fluctuations were easily seen. The dependence of these readings on pressure is not simple, so it was found to be easier to make the vapor pressure measurements by conventional monometry than to calibrate and then use the TI gages. However, above the λ point, where the He^4 bath and thus the vapor pressure bulb could not be kept at a quite constant pressure and temperature, the TI gages were useful in two ways: first, by displaying the pressure fluctuations, they made it possible to measure the height of both sides of the Hg manometer while the pressure was at the same value; second, by recording the pressure as a function of time they made possible small corrections for the fluctuations when Ge thermometer resistances were not measured at the same times as the vapor pressure. These corrections cannot be completely accurate since they assume linearity of the gage readout with pressure over the pressure range of the fluctuation, but none were more than 1.6 mK and most were much less. No correction for

thermomolecular pressure gradients was necessary because of the large size of the tubes used.[66] No correction was made for the pressure gradient caused by the difference in the weights of the hot and cold columns of gas, since the magnitude of the correction was estimated to be less than 0.5 mK,[67] and the exact magnitude of the correction cannot be calculated without more knowledge of the temperature gradient in the cold column of gas than was readily available.

Magnetic Thermometry

T_η is not only intended to be identical to T_{58} between 1.2 and 4.2 K, it is also directly based on T_{58} below 1.2 K. This extension of T_{58} is accomplished by measurement of the susceptibility of the CMN salt, known to obey the Curie law in the temperature region of interest. A mutual inductance bridge was used to measure the susceptibility, and temperatures were calculated from $M = M_\infty + A/T$, where M is the mutual inductance in arbitrary units. The two constants, M_∞ and A, are determined from measurements in the 1.2 to 3 K region, where T is already defined by vapor pressure measurements. M is plotted against 1/T in this region, and the best straight line through the points defines M_∞ and A. These constants and the measured values of M are then used to define T below 1.2 K. In the two calibrators referred to above, the temperature scale is extrapolated to 0.26 K in this manner. Thermometers used below 0.26 K have their calibration extended to lower temperatures by the same technique. Care must be taken in making the measurements and in defining M_∞ and A since small errors in these constants can cause

major errors in the definition of T at the low temperature end of the extrapolation. Accordingly, all the susceptibility data in the 0.26 to 3 K region were taken within 14 hours, during which mechanical jarring of the cryostat was avoided and the temperature of the He^4 bath was kept constant at 1.2 K. One transfer of liquid He^4 to the bath was necessary in the middle of this period. Measurements were not resumed until the bath temperature had returned to 1.2 K.

Pt Thermometry

Between 1.5 and 30 K, T_η is based on T_{55} through comparisons with a Pt thermometer calibrated by the National Bureau of Standards. The Pt thermometer was also used to determine the reference temperature (near 20 K) of the gas thermometer, which was used in the 4.2 to 20 K region. The gas and Pt thermometers agree to within their combined precision above 15 K but diverge below. Where they disagree, the gas thermometer was used to define T_η.

Gas Thermometry

The gas thermometer measurements used were done some years ago and have not been repeated, because of the difficulties of measurement. The thermometer was filled with one atmosphere of He^4 gas at 20 K, which minimized errors in pressure measurement but required corrections of 4.5% at 4.2 K for the non-ideality of the He^4 gas. Since the virial coefficients of He^4 gas are not well known, this correction is expected to be the main source of error in the measurements. Keesom's "adopted

values" of the virial coefficients[68] have to be used above 5 K, since they are the only self-consistent values in the 5 to 20 K region which are closely spaced enough to permit interpolation.[69] Below 5 K, the Keller[70] experimental values and the Kilpatrick et al.[71] theoretical values are useable, but a smooth transition from the Keesom values is possible only to those of Kilpatrick et al. and not to those of Keller. The Kilpatrick et al. values were used below 5 K. This gives a temperature scale between 4.2 and 20 K which is smooth in relation to magnetic scales[72] and to T_{65}. However, it is 4 mK below T_{58} at 4.2 K. In order to make T_η smooth through the 4.2 K region, the deviation curves of T_{58}, T_{65} and this gas thermometer scale from a fit equation for Ge thermometer 897 were all plotted together. T_η was drawn as a deviation curve which joined smoothly onto that of T_{58} at 4.2 K, joined smoothly onto that of the gas thermometer scale at 15 K (where it and T_{55} agree), and was smooth with respect to both T_{65} and the gas thermometer scale between 4.2 and 15 K.

Going to a lower filling pressure for the gas thermometer and thus reducing the magnitude of the virial coefficient correction would not necessarily ease the problem of matching the temperature scales at 4.2 K. Rogers et al.,[73] who used the same virial coefficients and also took their reference temperature from T_{55}, but who worked at pressures $\frac{1}{5}$ as high and used a single bulb gas thermometer, found their temperature scale to be 8 mK above T_{58} at 4.2 K. Further, the magnetic thermometry of Cetas and Swenson[72] indicates that T_{55} and T_{58} are not thermodynamically consistent, though it shows that a temperature scale based on T_{55} is only 5 mK above T_{58} at 4.2 K.

Acoustic Scale

The acoustic scale used for compsrisons with T_η was not obtained directly from NBS. A Ge thermometer calibrated by CryoCal against a thermometer calibrated on T_{65} by NBS was purchased from CryoCal for use until one could be obtained from NBS. The difference between the CryoCal "T_{65}" and T_η at 4.2 K agrees with the published difference between T_{65} and T_{58}[74] to within 0.5 mK.

Smoothness of Heat Capacities

T_η is the result of a series of new measurements and of recalculations which were initiated when it was found that heat capacities calculated on the earlier laboratory temperature scale, T_δ, were questionable near 4.2 K. In particular, the heat capacity of pure Cu had a sharp peak near 5 K in a plot of its deviation from the reference equation of Osborne et al.,[75] and the heat capacity of pure W had a negative T^5 term. The new measurements showed that T_δ differed from T_{58} by 4 mK at 4.2 K, apparently because a leak in the vacuum jacket of the vapor pressure bulb introduced errors in the earlier vapor pressure measurements. By comparison, when T_η is used to calculate heat capacities from the same data, the W has a positive T^5 term, and the peak in the Cu deviation plot is reduced in size (and altered in shape). T_η has not been directly defined or smoothed via heat capacity measurements; although sharp variations in the size of the degree on a temperature scale will produce anomalies in the heat capacity, such anomalies may also be produced by impurities in the "pure" material.[76]

The paper by Holste et al.[77] gives a useful discussion of this problem and of the effects on heat capacities of changing temperature scale.

Standard Ge Thermometers

All of the temperature measurements described above are preserved on the standard Ge thermometer, Honeywell[78] number 897, permanently mounted on the calibrator. A second, higher resistance Ge thermometer is also permanently mounted and is calibrated above 2 K. Periodic comparisons of the calibrations of the two thermometers provide checks for any loss of calibration with aging. Over the past 6 years these two thermometers have continued to agree with each other to within the precision of the calibration points, approximately 0.1%.

Mathematic Representation of the T_η Scale

The data which define the temperature scale are fitted to an equation of the form $1/T = \sum_{i=0}^{n} A_i(\log R)^i$, where R is the thermometer resistance. (No satisfactory theoretical relationship exists between R and T, but in practice the above equation gives a satisfactory fit.) For thermometer 897 and temperature scale T_η, a 10 term fit was used for the 0.26 to 30 K temperature range. Fits with more terms will give smaller average deviations of the data points from the fit equation, but are less satisfactory in other ways which will be discussed later. The percent deviations, Δ, of the data points from the equation are then plotted against temperature and a smooth curve drawn through them. This curve is represented by a table which, together with the equation, defines the temperature scale to about 1 part in 10^5.

In heat capacity measurements, where accuracy in measuring temperature differences is more important than accuracy in measuring the absolute temperature, errors in the slope of the smooth curve on the Δ plot are the errors most likely to affect the accuracy of the heat capacities. Such errors are especially likely where the slope is steep and where it changes rapidly in rapid oscillations about zero. Both problems are most likely at the extremes of the temperature range of the calibration, and can be partially reduced by extending the calibration to a broader temperature range than is covered in the heat capacity measurements. Reducing the number of terms in the fit reduces the number of oscillations, and weighting the points at the extremes of the fit makes the slopes at the extremes less steep.

Calibration of Working Thermometers

The thermometers used for measuring heat capacities are usually calibrated by comparison with thermometer 897 at calibration points spaced about (T/15) apart. Closer spacing is used at the temperature extremes of the calibration. When the calibration has to be extended below 0.26 K, the thermometer is mounted in an adiabatic demagnetization cryostat, in thermal contact with a CMN salt. Mutual inductance measurements are taken and used as described earlier. The constants in the equation relating M to T are defined from T_η as carried on the thermometer in question, and measurements at temperatures down to 0.26 K are used in defining them.

Specifically, the 782 was originally calibrated against the standard 897 from 0.3 to 30 K. Its calibration was extended down to 0.2 K when it was found that the rapid oscillations at the low temperature end of its Δ plot rendered it virtually impossible to draw the Δ curve well enough to avoid introducing a spurious anomaly in the heat capacity near 0.4 K. The problem may have been increased by a carry-over to the 782 of errors in the temperature scale carried at that time by standard 897, T_8. Hindsight suggests that with the elimination of problems in the temperature scale, going to a fit of slightly fewer terms and giving extra weight to the lowest temperature points probably would have cured the problem with the 782 without any need for further calibration. The 1751 was calibrated between 0.3 and 3.0 K against standard 897. Its calibration was then extended down to 0.058 K so that it could be used for heat capacity measurements in an adiabatic demagnetization cryostat.

Samples and Measurements

LU

All experiments coded with the letters LU were done on pieces cut from a 100 g, $\frac{1}{2}$" diameter rod of Ce of nominal 99.9% purity purchased from the Lunex Company.[79] A mass spectrographic analysis indicates a purity of less than 99.8% for these pieces. Table I gives the detailed impurity analyses of those Ce samples for which it is available. The mass spectrographic analyses searched for all stable elements but were unable to measure the concentrations of elements of atomic number less than 9.

The rod of LU Ce was cooled from the melt in a Cu mold, a very fast cooling but not quite a quench. Piece A, when first taken below room temperature, was cooled to 100 K in 45 minutes, then cooled more slowly to 0.3 K, after which a heat capacity measurement was taken from 0.4 to 24 K. This rapid initial cooling through the $\gamma \rightarrow \beta$ phase transition region into the region where the α phase is the thermodynamically stable phase minimized the amount of β phase in the sample during the first measurement. All other coolings for and all rewarmings from a measurement on piece A passed through the critical 100 to 300 K region in 4 to 8 hours. The second measurement was done after one such warming and cooling, with no other thermal treatment of the sample. The third measurement was done after the sample had been warmed to room temperature, cooled to 200 K for 5 hours, returned to room temperature, then cooled to 0.3 K. The fourth measurement was done after a similar procedure

with the temperature held at 230 K for 5 hours. Neither of these attempts to increase the amount of β phase in the sample by leaving it in the region of β phase stability was notably successful, so the more standard technique of cycling the sample was resorted to. The sample was placed in a sealed container under N_2 exchange gas and cycled between room temperature and 77 K, with each cycle taking 30 to 40 minutes. The fifth measurement was taken after 10 such cycles, and the sixth after 30 more. Fifty additional cycles were done before the seventh measurement but they took only 10 minutes each and were too rapid for the thermal contact between the sample and its container, so that the thermal history of the sample during these cycles is unknown. Less β phase was detected in the seventh measurement than in the sixth. After this, the slower thermal cycling was resumed, and an eighth measurement done after 50 cycles, then a ninth after 100 more cycles. The piece was then machined to a smaller shape and a tenth measurement, the first from 0.08 to 0.8 K, taken. The eleventh and final measurement was taken after the sample had been exposed to the air and allowed to oxidize freely for two months. Piece B was measured only once, for which it was cooled through the 300 to 100 K region in 3 1/2 hours.

RC

All experiments coded with the letters RC were done on a piece cut from a 5/8" diameter, 3" long rod of Ce of nominal 99.9% purity purchased from Research Chemicals.[80] The mass spectrographic analysis indicates a purity of less than 99.9%. The rod was cooled slowly from the melt

in a graphite mold. The piece measured was taken from room temperature to 77 K in 3 hours, then taken to 0.3 K and measured first in zero field and then in a 60.5 kOe field. It was warmed, held for 6 hours at 200 K, and cooled before the second measurement in the same way the LU Ce was treated. The third measurement was done after no further thermal treatment except warming to room temperature and cooling down again.

JMA and JMB

These codes refer to 2 different Ce samples of nominal 99.99% purity purchased at different times from Johnson, Matthey and Company.[81] Mass spectrographic analyses show JMA to be less than 99.9% pure and JMB to be less than 99.8% pure. Both were cooled from the melt in a few minutes in a water cooled Cu mold. JMA, for its first and only measurement, was cooled through the 300 to 100 K region in 6 hours. JMB was cooled through this region in 12 hours, and 2 heat capacity measurements were taken, one in zero field and one in a 9.4 kOe field, while the sample remained below 30 K.

For ease of comparison, the comparable information on samples used by other experimenters and referred to in this work is summarized here.

PGβ

PGβ refers to the heat capacity measurement on a 91 ± 5% β sample of Ce by Panousis and Gschneidner.[32] This Ce is 99.9% pure. These authors subjected it to a high temperature annealing and cycling process

to increase the grain size, at the end of which it was air cooled from 975 K to room temperature. After this it was cycled 30 times between room temperature and 4.2 K before its heat capacity was measured.

PGα

PGα refers to the data on a sample of Ce described by Panousis and Geschneidner[32,82] as 100% α phase but appearing to have at least 3% β phase. The sample is 99.9% pure. The rate at which it was cooled from the anneal is not given. It was put under 10 kbar pressure at room temperature, cooled under pressure to 77 K, returned to 1 atm pressure and drilled and tapped at 77 K, then cooled to 4.2 K for the heat capacity measurement.

PR

PR refers to the 1.5 to 20 K data of Parkinson and Roberts[83] on a Ce sample less than 99.6% pure. Only the impurities Li (0.4%) and Fe (0.04%) are reported. Significant concentrations of the other rare earths and an over-all purity less than that of the more recent LO can be expected in a Ce sample of this age.

PSS

PSS refers to the 20 to 200 K data of Parkinson, Simon, and Spedding[43] on a Ce sample whose purity is less than 99.5%. Reported impurities are: Mg 0.25%, Ca 0.125%, Fe 0.02%, other rare earths less than 0.1%. Since this is the oldest of the Ce samples it is almost certainly the least pure.

LO

LO refers to the 0.4 to 4 K data of Lounasmaa's[84] "experiment I" on a less than 99.6% pure Ce sample. The sample was cooled from the melt to room temperature in about 1 1/2 hours. It was then slowly cycled between 293 and 77 K 4 times before the heat capacity was measured.

PHS

PHS refers to the 0.3 to 6 K data of Phillips, Ho, and Smith[23] on a sample of 100% α Ce at approximately 11 kbar. The sample is 99.9% pure. Details on the thermal treatment are not given.

RESULTS

Qualitative Description

The set of heat capacity measurements reported here incorporates several tactics for separating the contributions to the total heat capacity of Ce. First, a single sample of Ce was measured many times, with its mole fraction of β phase, χ_β, different each time. This showed the effects on the heat capacity of changing χ_β without changing sample dependent factors such as the purity of the Ce. Second, several different samples of Ce were each measured at least once, permitting analyses of the effects of the sample dependent factors. Third, one sample was remeasured after being allowed to oxidize heavily, so that contributions from the slight surface oxidation present in all samples could be estimated. Fourth, high magnetic fields were applied to 2 samples already measured in zero field, in order to determine the field dependence of the heat capacity. Table II lists all of the heat capacity measurements referred to, with the temperature range of the measurement, the χ_β, the temperature of the observed maximum in the β ordering peak (on a plot of C/T vs. T), and the extrapolated γ_o.

A sample of Ce containing both α and β phases has a large heat capacity throughout the entire 0.08 to 24 K range. Near 12.5 K, the heat capacity is dominated by the antiferromagnetic ordering peak of the β phase. As many as 3 other peaks are observable, all very much smaller than the β peak. They occur near 0.15, 0.9, and 6 K. A small

hyperfine contribution is noticeable below approximately 0.2 K. As the χ_β of a sample is increased, the total heat capacity increases at all temperatures between 0.08 and 24 K, the β peak increases in size, and the 0.9 and 6 K peaks remain approximately constant (figures 3 through 5). The behavior of the 0.15 K peak is irregular. Different samples with comparable χ_β's have similar but not identical heat capacities (figures 6 through 15). The differences are most noticeable below approximately 5 K, but amount to only a few percent of the total heat capacity. The 0.9 and 6 K peaks have different sizes and shapes in different samples, and the β peak has a somewhat different shape. Two samples, the PGα and the JMA (to a lesser extent), have anomalously high heat capacities above approximately 17 K. Heavy surface oxidation on the Ce does not affect its heat capacity above 0.4 K (figure 17). Magnetic fields do affect it. The application of a 9.4 kOe field raised the total heat capacity of JMB Ce between 0.4 and 2 K, and lowered the temperature of its 0.9 K peak (figure 14), but did not change the heat capacity from 2 to 5 K (the high temperature limit of this measurement). A 60.5 kOe field lowered the total heat capacity of RC Ce between 0.4 and 2 K, probably lowered its 0.9 K peak (figure 12) and lowered, broadened, and decreased the apparent size (by less than 5%) of the β peak (figure 18). A 2 kOe field had no detectable effect on the PHS pure α Ce.[23]

The size of the β peak is, of course, proportional to χ_β. Its width and temperature are not quite constant. As χ_β increases from 0.30 to 0.80 in LU Ce, the width of the peak increases by at least 1 K

and its temperature decreases by at least 0.5 K. Different Ce samples of comparable χ_β have differences of a few tenths of a degree in the width and temperature of their β peak. The 60.5 kOe field does not noticeably change the temperature of the peak but does increase its width by 0.6 K.

The minor peaks at 0.15, 0.9, and 6 K are all significantly sharper than Schottky anomalies, and are thus probably ordering peaks. Only 3 experiments were done in the temperature region of the 0.15 peak, and its size, width, and temperature are different in all 3 (figures 19 and 20). These parameters have no simple dependence on χ_β or on what sample is measured. The size is proportional to the estimated amount of oxide on the surface of the Ce, but this has not been confirmed by measuring a heavily oxidized sample at this low a temperature. At most 0.003% of the total Ce in the samples is associated with this peak. The 0.9 K anomaly has been detected in all samples except PHS measured to that low a temperature (figures 12 through 16). Its width and temperature change slightly with χ_β, but its size remains constant (figure 21). Heavy oxidation does not affect this peak. Its size, width, and temperature are different in different samples of Ce, but are not dependent on the rate of cooling of the sample from the melt (and thus presumably not dependent on the grain size or on the degree of concentration of the impurities at the grain boundaries). The size is roughly proportional to the total amount of impurities in the sample, though such a conclusion must be tentative in view of the inadequate data on the concentrations of H and O impurities. The peak's decrease

in temperature in a magnetic field shows it to be caused by an antiferromagnetic ordering. It represents at most 0.06% of the total Ce in any sample (less if something other than Ce is causing or helping cause it). The 6 K peak has been detected only in the PR and LU samples (figures 4 and 11). The size, width, and temperature of this peak are insensitive to χ_β (figure 22) and to the amount of oxide coating. They are different in different samples, having the same lack of dependence on the rate of cooling and the same rough proportionality to the amount of impurities as is seen for the 0.9 K peak. In LU Ce, this anomaly represents less than 0.06% of the total Ce. It represents less than 6% of the PR Ce.

A small nuclear hyperfine heat capacity (approximately $4 \cdot 10^{-3}$ mJ/K^4·mole) associated with some of the impurities in the samples is visible below approximately 0.2 K. It is slightly larger in LU than in RC Ce (figure 19).

Data Analysis

Phase Composition

Since it is generally infeasible to measure the phase composition of Ce samples directly during heat capacity measurements, that information has to be derived from the heat capacities thermselves. Two methods of deriving it have been found useful and reasonably accurate. The first is based on the fact that the 12.5 K peak in the heat capacity of Ce is caused by ordering in β Ce only,[12] so that the entropy associated with it, S_M, is strictly proportional to χ_β. Ideally, S_M can be calculated from the known degeneracy of the ground level of the system undergoing ordering. In practice, there is sufficient uncertainty as to how much of the total entropy should be assigned to the magnetic ordering that it is necessary to develop 1 or more reasonable definitions of S_{Mi} for a system of unknown χ_β and compare that S_{Mi} with the S_M defined in the same way for a measurement of pure β Ce or of Ce of known χ_β. The second method of determining χ_β is based on the ideal equation representing the total heat capacity observed in experiment i:

$$C_i(T) = \chi_{\beta i}\, C_\beta(T) + (1 - \chi_{\beta i})\, C_\alpha(T) \qquad (4)$$

where C_β and C_α are the heat capacities of the pure β and pure α phases. This equation assumes that no other phase of Ce is present in significant amounts, and neglects contributions from impurities. Once C_α and C_β are known, $\chi_{\beta i}$ can be derived. Since no pure α or pure β Ce samples have been measured at zero pressure, C_α and C_β must be derived from data on experiments for which χ_β is known.

The χ_β of the PGβ sample was measured dilatometrically to be 0.91 ± 0.05,[32] making it possible to use the data on this sample for the $\chi_{\beta i}$ determinations based on S_{Mi} comparisons. It can also be used as one of the 2 C_i needed to define C_α and C_β in equation 4. The best second C_i appears to be the heat capacity of PGα Ce after its χ_β has been determined by S_{Mi} comparisons. Its χ_β of approximately 0.03 is sufficiently small that the $\chi_{\beta i}$'s derived for other experiments from equation 4 are not sensitive to the exact choice of χ_β for PGα. Thus the χ_β's determined by the 2 different methods are determined essentially independently of each other, and the agreement between them is evidence for their validity.

In estimating $\chi_{\beta i}$ from S_{Mi}, 3 different definitions of S_{Mi} were used. For a given experiment, the 3 χ_β's estimated agreed with each other to within 7%.

In estimating $\chi_{\beta i}$ from equation 4, calculations were restricted to the 5 to 11 K temperature range. Below 5 K, equation 4 does not hold, primarily because of the broad peak near 0.9 K, which is not a part of C_α or C_β. Above 11 K is a region where the C_i change very rapidly with temperature near the β ordering peak, so that they are not well known between experimental points. Above this region the heat capacity of the PGα sample is anomalously high and not in accord with equation 4. For a given experiment, the χ_β's estimated from equation 4 in this restricted temperature range agree to within 3% and fall at the high end of the range of values determined by S_{Mi} comparisons.

Calculating S_{Mi} is tedious and less precise than using equation 4, and having to restrict the use of equation 4 to between 5 and 11 K is limiting. For these reasons, the LU experiments of highest (excluding the experiment where the Ce was heavily oxidized) and lowest χ_β were used as secondary standards for determining the χ_β of other experiments, after their χ_β's were carefully determined from both S_{Mi} and equation 4. The precision of the comparisons of other experiments with these 2 is 3% or less (outside of the regions of the 0.9 and 6 K peaks) for all experiments except the ones on PGα and JMA. The χ_β of JMA was chosen to be the one estimated from S_{Mi}. The χ_β's of all experiments are reported in Table II. Note that the one calculated for LO Ce is 0.35, in good agreement with Lounasmaa's estimate of 0.40, which is based on an x-ray diffraction measurement done after the sample was warmed back to room temperature.[84]

Low Temperature Contributions

The magnetic and crystal field heat capacities of Ce are expected to be very small at low temperatures. When this is the case, $C = C_E + C_L$ and $C/T = \gamma_o + AT^2/\theta_o^3$. (The non-linearities of the enhancement effects in γ_o are at most a small percentage of its total value at low temperatures.) Experimental data plotted as C/T vs T^2 will fall on a straight line with intercept γ_o and slope = A/θ_o^3. This method of determining γ_o and θ_o requires no a priori assumptions as to their magnitudes.

When the low temperature heat capacity data on Ce is plotted as C/T vs T^2, they fall on a straight line except where the contribution of the

0.9 K peak is significant (figures 12 through 16). In the LU and LO experiments, where the peak is narrow and where good data could be obtained on its low temperature side, this data appears to fall very close to the same straight line used to approximate the data on the high temperature side of the peak. (In the JMB experiments and in the RC experiment in a 60.5 kOe field, the lowest temperature data falls below the straight line. This is not believed to be significant, since the long relaxation times of the JMB sample reduce the accuracy of the measurements, while the uncertainties in the addendum in 60.5 kOe are sufficient to explain the RC data.) For a given χ_β, the γ_o's determined for different Ce samples vary by less than 10%. The variation appears attributable to the uncertainties introduced into the extrapolation by the 0.9 K peak and to the small uncertainties in χ_β. The γ_o's of pure α and pure β Ce are estimated to be 22 and 54 mJ/mole·K^2, respectively. The θ_o's are 56 and 125 K, respectively, with uncertainties of approximately 10 K.

The heat capacity of PSS Ce, with $\chi_\beta = 0.50$, shows a C_L comparable to that of La over a very wide temperature range,[43] which is the expected behavior for β Ce. This means θ_o for β Ce should be approximately 152 K, not 56 K. In that case, the slope actually observed for β Ce is approximately 6 times that expected. The most probable interpretation of this behavior is that C_M is making a large contribution to C at low temperatures. When there is no energy gap in the spin-wave spectrum, $C_M \propto T^3$, and thus it does not interfere with the determination of γ_o. Only when there is an energy gap is the extrapolated γ_o likely to be wrong. The large contribution of C_M to C at low temperatures (to 0.08 K) strongly implies

that the gap is nonexistent or very small, but the lack of dependence of the apparent γ_o on the applied magnetic field implies that the gap is very large (a 60.5 kOe field should induce a gap of approximately 8 K). In the absence of knowledge of the size of the gap and of the temperature dependence of C_M, it is difficult to know how much confidence should be placed in the extrapolated γ_o's reported in table II.

Rosen reports a θ_o of 139 K for a mixed phase sample of Ce,[85] and estimates it to be accurate to 0.5 K. This value is an accord with the estimated θ_o's of 125 K for α Ce and 152 K for β Ce if the χ_β of his sample was approximately 0.5, a likely value.

High Temperature Contributions

The heat capacity of pure α Ce can be extrapolated from the LU experiments once their $\chi_{\beta i}$'s are known. This heat capacity has only lattice and electronic contributions, and its C_E is a small percentage of C for most of the 0.4 to 24 K range (0.3% at 22 K, 2% at 10 K, 14% at 4 K), so that C_L can be determined with reasonable accuracy. For the calculation, γ_o was rounded to 20 mJ/mole·K^2. This value is believed to be accurate to within 10 to 20%, in view of the fact that the T^3 heat capacity extrapolated for α Ce does not show (and should not show) any contribution from C_M. The $\theta(T)$'s calculated for α Ce are shown in Table III. The low total heat capacity below approximately 6 K and the uncertainties in γ_o can lead to considerable errors in θ at low temperatures. However, it is clear that above approximately 10 K the C_L of α Ce is lower than that of La,[40] and thus its θ is higher. Apparently this does not hold

below 10 K, where the θ_o of α Ce is less than that of La and presumably less than that of β Ce.

The entropy of magnetization in β Ce may be calculated from $S_M = S - (S_E + S_L + S_C)$. The calculations of Bleaney[42] (corrected for χ_β) were used to approximate S_C. For the LU experiment with $\chi_\beta = 0.80$, S_L was approximated by the S_L of La[40] and S_E was approximated by $\gamma_o \cdot \Delta T$. For the LU experiment with $\chi_\beta = 0.30$, the heat capacity of pure α Ce was used for $S_L + S_E$. In the former case, both S_M (16 K) and S_M (25 K) were found to equal 0.50 R ln 2 per mole β Ce. In the latter case, S_M (16 K) was calculated to be 0.43 R ln 2 while S_M (25 K) was 0.81 R ln 2. By 16 K, S_M should be on the order of 90% of its total value, and by 25 K, twice T_N, S_M should be essentially 100% of its total value. Clearly this is not the case. The data can be force-fit to give S_M (16 K) = 0.9 R ln 2 and S_M (25 K) = R ln 2 only by assuming that S_C is negligible below 25 K and that the true (or the average) γ value of β Ce is less than half the apparent γ_o.

Secondary Contributions

The nuclear hyperfine heat capacity can be calculated only approximately because of its small size and the interference of the 0.15 K anomaly, but this is not a problem because its interference with the extrapolation of data to zero K is negligible. The value of C_N is approximately $4 \cdot 10^{-3}$ mJ/mole K^4. It is slightly larger in LU Ce than in the purer RC Ce.

The size of the 0.15 K anomaly appears to be proportional to the amount of oxidation of the surface of the Ce sample, though this has not been confirmed by measurements of a heavily oxidized sample at these temperatures. Its shape indicates that it is an ordering peak of some sort.

The origin of the 0.9 and 6 K peaks remains less than certain. Such small, sample dependent peaks are common to the rare earths,[86-90] and might be a reflection of the problems in purifying them, or might be caused by ordering transitions in metastable phases (the phases can be stabilized by impurities or strains). Direct ordering of the impurities seems unlikely, since the presence of the peak does not depend on the impurities having had an opportunity to become concentrated along the phase boundaries. In Ce, the fcc γ phase is a likely cause of one of the two peaks: it is expected to be present in small amounts and to order. An hcp phase, essentially a region of stacking faults in the dhcp β phase, is a possible source of the second peak.

Discussion

α Ce

The γ_o value of 22 mJ/mole·K^2 for α Ce is high for an element, approximately 16 mJ/mole·K^2 higher than expected for a metal with an s-d conduction band and with a valence of 3.61. This extra 16 mJ/mole·K^2 is attributable to the presence of the 4f electron, presumably in the predicted virtual bound state. Its size is in accord with the predicted 12 or 24 mJ/mole·K range of the f virtual bound state contribution.[28,29] The γ_o of the s-d conduction band was calculated by assuming that such a band has a γ_o which is linear in valence for valences between 3 and 4, and that its γ_o is 11.5 mJ/mole·K^2 (the γ_o of fcc La[91]) when its valence is 3 and 2.2 mJ/mole·K^2 (the γ_o of hcp Hf[91]) when its valence is 4. This assumption of linearity has not been confirmed for valences between 3 and 4 by studies of alloys of intermediate valence, but it is known to be a good approximation for valences between 5 and 6 and between 7 and 8.[92] The zero pressure, zero temperature valence of α Ce was calculated from the equations describing the virtual bound state model:[28,29]

$$N_f(\epsilon_F) = 7\,\Gamma/(\pi E^2), \quad n = 7\,\Gamma/(\pi E)$$

$N_f(\epsilon_F)$ is the density of f states at the Fermi surface, calculated from the f contribution to γ_o and from equation 1; Γ is the half-width of the virtual bound state, estimated to be 0.01 eV from IR absorption measurements;[93,28] E is the height of the virtual bound state above the Fermi surface; n is the number of f electrons, equal to 4 minus the valence.

At zero pressure and temperature, E is calculated to be 0.057 eV, and n to be 0.39.

The γ_o value for α Ce at 11 kbar is 11.3 mJ/mole·K^2,[23] of which approximately 7 mJ/mole·K^2 is attributable to the f contribution. This indicates that the valence of the α Ce has been raised to 3.74 by 11 kbar, and E is raised to 0.087 eV. This low-temperature pressure dependence of the valence calculated from the pressure dependence of γ_o is approximately twice as great as the room temperature pressure dependence calculated from the lattice constants.[14]

Although the virtual bound state model for the f level has predicted the electronic properties of α Ce essentially correctly, it appears less able to predict its unusual lattice properties. At zero pressure, α Ce has a θ_o of approximately 125 K, apparently significantly less than the θ_o of the nearly trivalent β Ce, and certainly not appreciably more than that of β Ce. By contrast, the θ_o of tetravalent Ce should be approximately 180 K, based on the assumption that it will be as much larger than the θ_o of its trivalent neighbor La (θ_o = 140 K for fcc La[91]) as the θ_o of tetravalent Hf (θ_o = 252 K[91]) is larger than that of its trivalent neighbor Lu (θ_o = 210 K.[94] Both are hcp). The alloy studies on the variation of θ_o with valence[92] are unfortunately of limited usefulness for assessing the behavior of the Ce phases because the process of alloying changes θ_o even when the valence is not changed. To the extent that the behavior of pure metals can be extrapolated from that of alloys, the studies appear to indicate a non-linear dependence of θ on valence. In this light, there exists some possibility that the θ_o of 125 K is

reasonable for α Ce with a valence of 3.61. The alternative possibility is that the 0.61 electron is not yet fully in the s-d band, so that the effective valence for the lattice binding forces is less than that for the electronic density of states. If this is the case, the electronic transition which occurs at the α-α' phase transition could be associated with a transition to full s-d character (and full participation in the lattice binding) of the originally 4f electron.

The 11 kbar θ_o value of 200 K for α Ce[23] is very approximate, because of the experimental problems involved in measuring heat capacities at high pressures. If the θ_o of α Ce is actually anywhere near this high at 11 kbar, it implies a far more rapid change in θ_o with pressure than can be explained by the slight change in the valence.

β Ce: Electronic Properties

The γ_o value of 54 mJ/mole·K^2 observed for β Ce is unlikely to be the result of a large contribution to the electronic density of states by the f level, as calculated by Rocher,[1] since the room temperature γ value, γ_{300}, observed for γ Ce is 7.24[95] to 7.5[2] mJ/mole·K^2. This γ_{300} is one of the lowest observed for the trivalent rare earths,[2] making it doubtful that even the small (1.2 mJ/mole·K^2) f contribution calculated by Coqblin and Blandin[28] is present. The $\gamma(T)$ of β Ce should be comparable to or smaller than that of γ Ce: the 2 phases have the same valence, the entropy change at their phase transition is too small to include any significant change in electronic entropy,[7] and the γ_o of dhcp La is 2.1 mJ/mole·K^2 lower than that of fcc La.[91] Nor is it likely

that the "lattice softening" observed in the elastic properties of γ and β Ce at low temperatures[15] corresponds to a valence increase large enough to significantly increase the f contribution to γ_o: The $\Delta\ell/\ell$ observed for γ Ce between 120 and 300 K[7] corresponds to a coefficient of thermal expansion of $8 \cdot 10^{-6}/K$, intermediate between that of Pr ($6.8 \cdot 10^{-6}/K$[96]) and that of Nd ($10.0 \cdot 10^{-6}/K$[96]). An increase in valence tends to contract the lattice, giving too high a coefficient of thermal expansion. The coefficient observed for Ce is at most 20% high.

The discrepancy between the estimated γ_{300} of β Ce and the apparent γ_o implies that if the γ_o is valid, an important temperature dependent enhancement effect is occurring. The phonon enhancement factor $\lambda_p(T=0)$ is calculated to be 0.7 to 2.5 for Sc and Y.[97] If Ce has a comparable λ_p, and if γ_{300} is approximately equal to γ_{bs}, then an enhancement of 5 to 18 mJ/mole K^2 at zero K can be expected from this contribution. The magnon enhancement factor $\lambda_m(T=0)$ is believed to be approximately 1.0 and insensitive to the strength of the magnetic exchange.[34] When this effect is included, the total expected enhancement to γ_{300} at zero K becomes 12 to 25 mJ/mole·K^2. Thus γ_o can be appreciably larger than γ_{300}. Possibly further theoretical work will show λ_m to be larger than 1.0 in some cases. At the present stage of knowledge, it cannot be definately said whether the γ_o of β Ce reflects the electronic properties alone or whether it contains some field-independent contribution from C_M.

Most of the other magnetic rare earths have the same ambiguity in their γ_o's as does β Ce. Their experimental heat capacities show a much larger linear term at low temperatures than at room temperature, which

can be ascribed entirely to γ_o or partially to C_M, but the justification for either interpretation is inconclusive. The data are summarized in Table IV. The large linear terms do appear to have some association with the magnetic properties of the elements and perhaps also with the f character of their magnetism, in view of the fact that such terms are not found elsewhere in the periodic table[91] (with the possible exception of the actinides) and are not found in the nonmagnetic rare earths La, Yb, and Lu. This may mean that the relatively low ordering temperatures of the rare earths cause their C_M's to be large at low temperatures (so that an important linear contribution is possible, though this alone does not make it certain). Alternatively, it may mean that $\lambda_m(T=0)$ is larger than expected. This does not explain why the apparent size of λ_m varies so much among the rare earths. If the γ_o's of the nonmagnetic rare earths are used to approximate the band structure density of states with phonon enhancement, then λ_m varies from zero to 12. Whatever the source of its unusual size, the linear term shows no correlation with the type of magnetic ordering and little correlation with the ordering temperature. Further study would be valuable.

β Ce: Magnetic Properties

The entropy associated with the 12.5 K ordering peak in the β phase of Ce, S_M, is only 1/2 R ln 2. The experimental data can be force-fit to give S_M = R ln 2 only by assuming C_C to be essentially zero below 25 K and simultaneously assuming γ to be significantly less than the apparent γ_o. Heat capacity measurements have been done on hcp CeY

alloys,[32] and these also show an S_M of 1/2 R ln 2[103] per mole Ce. In the alloys, the Neel temperature T_N is moved to a lower temperature as the Ce is diluted by the non-magnetic Y, while C_C is to a first approximation unchanged, and C_L is slightly reduced. The effect on C_E is not known, but presumably it is decreased by the addition of Y with its much lower γ_o (8.2 mJ/mole·K[291]). The alloy with 31.4% Y has a T_N near 5 K, where both C_C and C_L are small. Force-fitting the data on this alloy to give S_M = R ln 2 per mole Ce requires the assumption that significant contributions to S_M occur at temperatures as high as 4 to 5 times T_N.

An S_M of 1/2 R ln 2 for a single ordering peak is what should be expected for an element with dhcp stacking. The theoretical treatment of the 2 non-equivalent lattice sites in the dhcp lattice predicts that they should have different behavior,[42] and this prediction is confirmed by the experimental data on the dhcp elements Pr and Nd. Only the sites of hexagonal symmetry order in Pr.[50] Both sites order in Nd, but the cubic sites order separately at a lower temperature than the hexagonal sites.[40,98] For both sites to order at the same temperature in β Ce would be anomalous behavior requiring investigation and an explanation.

Only the one 12.5 K T_N has been detected for β Ce by measurements of the heat capacity,[43] magnetic susceptibility,[6] and resistivity[20] of Ce. Two T_N's appear in the heat capacities of dhcp CeLa alloys.[104] The lower T_N, T_{Nc}, is the result of the transition which occurs at 12.5 K in pure Ce. This conclusion is based on the shape, S_M (approximately 1/2 R ln 2 per mole Ce), and temperature of the peak. The higher T_N, T_{Nh}, occurs at 12.5 K in the 21.1% La alloy, yet in CeLa as in CeY the

ordering transition must be lowered in temperature by the dilution of the magnetic exchange by the non-magnetic element. Judging by the fact that a given concentration of Y lowers T_{Nc} approximately 1.6 times as much as the same concentration of La, this dilution effect is less strong with La, possibly because of the partial f character of its conduction band.[29] The behavior of T_{Nh} in the CeLa alloys is unusual. The entropy per mole Ce associated with it appears to increase as the concentration of La increases. The magnetic susceptibility of the alloys[104] shows no anomaly for alloys containing little La, but shows a weak, antiferromagnetic-like anomaly at T_{Nh} when the La is 73.0% of the alloy. In short, the transition at T_{Nh} behaves like a magnetic ordering transition in a system with a singlet ground state, where the ratio of the magnetic exchange to the splitting between the ground and the first excited states is being increased as the concentration of La increases.[51] The quadrupole interaction must decrease more rapidly than the exchange interaction as the concentration of La increases.

Pure β Ce and Ce in dhcp alloys can have a singlet ground state on its hexagonal sites but not on its cubic sites.[45,46] The cubic sites have a doublet ground level and appear to be the sites ordering at 12.5 K in pure Ce. If the hexagonal sites have a singlet ground state it is because the electric quadrupole-quadrupole interaction has lifted the double degeneracy predicted by crystal field theory. With a singlet ground state, the hexagonal sites may not order at all.[51] The behavior of the CeLa alloys and the failure to detect two ordering transitions in pure Ce[6,20,43] are strong evidence for the existence of the postulated

singlet ground state. The latter is not evidence against ordering on the hexagonal sites of Ce, since no anomalies occur in the heat capacity,[40] magnetic susceptibility,[6] and resistivity[105] of Pr when ordering occurs on the singlet ground state of its hexagonal sites. Existing neutron diffraction measurements on Ce are inconclusive evidence on the point.[12] The elastic properties of Ce show an anomaly at 31 K[15] of the same type as is observed at T_N in Pr[96] and at the higher T_N in Nd.[96] (They fail to show an anomaly at 12.5 K in Ce[15] and at the lower T_N in Nd.[96]) The extrapolation of T_{Nh} in CeLa alloys gives a pure Ce T_{Nh} of 16 to 17 K, not 31 K. However, 31 K is about as much higher than the T_{Nh} of Pr as that T_{Nh} is above the T_{Nh} of Nd, so it does not appear to be unreasonably high. A third possible T_{Nh} is at 20 to 25 K, if the anomalous high temperature heat capacities of PGα and JMA Ce are assumed to be caused by T_{Nh}.

An entropy of 1/2 R ln 2 remains to be accounted for. This is that part of the entropy of the 4f electron which is not associated with either the traditional crystal field splitting[42] or the ordering on the cubic sites. It should be associated with the quadrupole contribution to the heat capacity or distributed between that contribution and the magnetic heat capacity of any ordering on the hexagonal sites. Accounting for this entropy does not require any revision of the model just developed for the hexagonal sites, but cannot be done exactly because of the large uncertainties in estimating C_L, C_E, and C_C (which is based on a fit to experimental data done with the assumption that the hexagonal sites had a doublet ground level[42]), and even in estimating the total heat capacity of β Ce above 25 K.

TABLE I

Impurity Analyses (atomic ppm)

Element	LU[a]	RC[a]	JMA[a]	JMB[a]	PAN[b]	LO[c]
H	e	e	e	e	417	30,500
C	e	e	e	e		8,400
N	e	e	e	e	40	440
O	(460)[d]	e	e	e	551	6,480
F	7	74	37			2,510
Na	61	91	12			
Mg	58	58	58	115	8	
Al	104	104	104		6	
Si	50	50	50		30.	
P	23	113	4			
S	4	22	4			
Cl	40	20	40			
K	54	36	36	72		20
Ca	18	18	280	350	7	30
Sc	3	3	3	3	4	
Ti	50	88	88	9		
V	3	3	3	3		
Cr	85	8	3	108	2	40
Mn	15	51	5	76		
Fe	106	100	25	75	40	370
Ni	91	36		24	10	70
Cu	1080	22	22	1550	4	
Zn	2	6	6		1	
Y	158	16	16	16	20	40
Mo						20
Ag	2		6			230
I	1					
La	134	10	151		10	4

TABLE I (continued)

Element	LU	RC	JMA	JMB	PAN	LO
Pr	12	10	25		10	
Nd	136	58	19	97	50	10
Sm	187					
Eu						170
Gd	42	67	45	36	40	20
Tb	4	176	18	9		
Dy	10	7	2	17	7	20
Ho	2	2	1	2	5	
Er	25	2	1	7	10	670
Tm		2	2			
Yb	5	1	1			
Lu	2	1	1			
Ta				58	30	80
W			1			
Pt			50			
Th	39	362			40	110
U	1	3	3			
Subtotal[f]	0.261%	0.162%	0.112%	0.257%	0.034%	0.441%
Total[g]	0.307%				0.134%	5.023%

[a] impurity analysis done mass spectrographically

[b] chemical analysis

[c] chemical analysis for H, C, N, O, and F, spectrographic analysis for the rest

[d] estimated by the supplier

[e] not measured; unless so noted, elements not reported were not detected in the mass spectrographic analysis

[f] total reported except for H, C, N, and O

[g] total reported; totals are non-equivalent because not all were analyzed for H, C, N, and O

TABLE II

Summary of Experimental Results

Sample	χ_β	γ_o $\frac{mJ}{mole \cdot K^2}$	β peak T (K)	T range (K)	special conditions
LU	0.30	31.7	12.9	0.4 - 23	
LU	0.34	32.9	——	0.08 -0.9	piece B
LU	0.38	34.6	12.5	0.4 - 22	
LU	0.42	35.4	12.5	0.4 - 22	
LU	0.45	36.4	12.5	0.5 - 24	
LU	0.50	38.4	12.4	0.4 - 23	
LU	0.62	42.6	12.4	0.4 - 24	
LU	0.59	40.9	——	0.04 - 7	
LU	0.65	43.2	12.4	0.4 - 23	
LU	0.80	47.6	12.4	0.4 - 23	
LU	0.82	48.2	——	0.08 -0.8	
LU	0.82	48.2	12.5	0.4 - 24	oxidized
RC	0.61	43.1	12.2	0.4 - 22	
RC	0.61	40.4	12.2	0.4 - 21	60.5 kOe
RC	0.63	44.0	12.2	0.4 - 24	
RC	0.63	46.0	——	0.08 -0.9	
JMA	0.57	45.3	12.1	0.04 - 23	
JMB	0.65	42.6	12.2	0.04 - 19	
JMB	0.65	44.0	——	0.04 - 5	9.4 kOe
PGβ	0.91	——	12.4	3 - 19	
PGα	0.03	——	(13)	2.5 - 20	
PR	0.88	——	12.3	1.5 - 20	
LO	0.35	37.1	——	0.4 - 4	
PSS	0.50	——	——		
PHS	0.00	11.3	——		11 kbar

TABLE III

Heat Capacity of α Ce

T(K)	C_α(mJ/mole·K)	θ(K)
0	0	125
2	40	73
4	140	101
6	282	114
8	584	120
10	1070	122
12	1740	124
14	2604	125
16	3552	127
18	4590	128
20	5640	130
22	6710	131

TABLE IV

Properties of the Rare Earths

	γ_{300}[b] (mJ/mole K)	apparent γ_o[d] (mJ/mole K)	T_N[i] (K)	T_C[i] (K)	low temperature magnetic structure
La		9.4[e]	—	—	none
Ce	7.5[c]	54[f]	?,12.5	—	complex antiferromagnetic
Pr	7.3	26.2	25,—	—	" "
Nd	8.6	58	20, 7.5	—	" "
Sm	11.5	12.4	14.8	—	" "
Eu[a]	3.7	12.1	90	—	" "
Gd	9.2	(11)[g]	292	293	simple ferromagnetic
Tb	12.2	10.4	229	221	" "
Dy	9.1	17.9	178.5	85	" "
Ho	7.9	50	132	20	conical ferromagnetic
Er	11.8	(9.1)[h]	85	19.6	" "
Tm	7.2	22.3	51-60	22	complex ferrimagnetic
Yb[a]		2.9	—	—	none
Lu		11.3	—	—	none

[a] divalent; the rest are trivalent

[b] reference 2

[c] fcc γ phase

[d] reference 99 except as noted

[e] reference 100, dhcp phase

[f] present work, dhcp β phase

[g] reference 101, not recalculated without a priori assumptions (probably would not be much changed)

[h] reference 102, not recalculated without a priori assumptions (could be higher than 9.1)

[i] reference 98

References

1. Y. A. Rocher, Advan. Phys. 11, 233 (1962) and Rare Earth Research III, L. Eyring ed. (Gordon and Breach, N.Y., 1965), p. 127.
2. K. A. Gschneidner, Jr., Rare Earth Research III, op. cit., p. 153.
3. J. G. Huber and M. B. Maple, J. Low Temp. Phys. 3, 537 (1970).
4. M. B. Maple, J. Wittig, and K. S. Kim, Phys. Rev. Letters 23, 1375 (1969).
5. B. Coqblin and C. F. Ratto, Phys. Rev. Letters 21, 1065 (1968).
6. J. M. Lock, Proc. Phys. Soc. (London) B70, 566 (1957).
7. K. A. Gschneidner, Jr., R. O. Elliott, and R. R. McDonald, J. Phys. Chem. Solids 23, 555 (1962).
8. A. Jayaraman, Phys. Rev. 137, A179 (1965).
9. E. King, J. A. Lee, I. R. Harris, and T. F. Smith, Phys. Rev. 1B, 1380 (1970).
10. K. A. Gschneidner, Jr., R. O. Elliott, and R. R. McDonald, J. Phys. Chem. Solids 23, 1191 (1962) and J. Phys. Chem. Solids 23, 1201 (1962).
11. J. Wittig, Phys. Rev. Letters 21, 1250 (1968).
12. M. K. Wilkinson, H. R. Child, C. J. McHargue, W. C. Koehler, and E. O. Wollan, Phys. Rev. 122, 1409 (1961).
13. K. A. Gschneidner, Jr., and R. Smoluckowski, J. Less-Common Metals 5, 374 (1963).
14. E. Franceschi and G. L. Olcese, Phys. Rev. Letters 22, 1299 (1969).
15. M. Rosen, Phys. Rev. 181, 932 (1969).
16. F. W. Clinard, Jr., J. Appl. Phys. 40, 3067 (1969).

17. B. L. Davis and L. H. Adams, J. Phys. Chem. Solids 25, 379 (1964).

18. R. I. Beecroft and S. A. Swenson, J. Phys. Chem. Solids 15, 234 (1960).

19. M. R. MacPherson, G. E. Everett, D. Wohlleben, and M. B. Maple, Phys. Rev. Letters 26, 20 (1971).

20. N. R. James, S. Legvold, and F. H. Spedding, Phys. Rev. 91, 1092 (1952).

21. C. J. Kevane, S. Legvold, and F. H. Spedding, Phys. Rev. 91, 1372 (1953).

22. Assuming 50% β phase on the first cooling. Gschneidner (reference 7) assumes 25% β, but in my experience this is too low.

23. N.E. Phillips, J. C. Ho, and T. F. Smith, Phys. Letters A27, 49 (1968).

24. T. F. Smith, Phys. Rev. 137, A1435 (1965).

25. B. T. Matthias, T. H. Geballe, and V. B. Compton, Rev. Mod. Phys. 35, 1 (1963).

26. H. Capellmann, J. Low-Temp. Phys. 3, 189 (1970).

27. J. Wittig, Phys. Rev. Letters 24, 812 (1970).

28. B. Coqblin and A. Blandin, Advan. Phys. 17, 281 (1968).

29. C. F. Ratto, B. Coqblin, and E. G. d'Agliano, Solid State Commun. 7, 1387 (1969) and Advan. Phys. 18, 489 (1969).

30. D. B. McWhan, Phys. Rev. B1, 2826 (1970).

31. C. J. McHargue and H. L. Yakel, Jr., Acta Met. 8, 637 (1960).

32. N. T. Panousis, Ph.D. Thesis, Iowa State University, Ames, Iowa, USAEC Report IS-T-398, 1970.

33. H. S. D. Cole and R. E. Turner, Phys. Rev. Letters 19, 501 (1967).

34. S. Nakajima, Prog. Theoret. Phys. (Kyoto) 38, 23 (1967).

35. L. C. David and S. H. Liu, Phys. Rev. 163, 503 (1967).

36. G. Grimvall, Solid State Commun. 7, 213 (1969).

37. G. Grimvall, Phys. Kondens. Materie 9, 283 (1969).

38. P. B. Allen and M. L. Cohen, Phys. Rev. B1, 1329 (1970).

39. W. L. McMillan, Phys. Rev. 167, 331 (1968).

40. O. V. Lounasmaa and L. J. Sundström, Phys. Rev. 158, 591 (1967).

41. H. Rosenberg, Low Temperature Solid State Physics (Oxford University Press, London, 1963).

42. B. Bleaney, in Rare Earth Research II, K. S. Vorres, ed., (Gordon and Breach, N.Y., 1963), p. 28.

43. D. H. Parkinson, F. E. Simon, and F. H. Spedding, Proc. Roy. Soc. (London) A207, 137 (1951).

44. R. J. Elliott, Phys. Rev. 124, 346 (1961).

45. G. T. Trammell, Phys. Rev. 131, 932 (1963).

46. B. Bleaney, Proc. Phys. Soc. (London) 77, 113 (1960).

47. H. Meyer and P. L. Smith, J. Phys. Chem. Solids 9, 285 (1959).

48. K. Nüra, Phys. Rev. 117, 129 (1960).

49. B. R. Cooper, Proc. Phys. Soc. (London) 80, 1225 (1962).

50. T. Johansson, B. Zebech, M. Nielsen, H. B. Møller and A. R. Mackintosh, Phys. Rev. Letters 25, 524 (1970).

51. Y. Wang and B. R. Cooper, Phys. Rev. 172, 539 (1968), and Phys. Rev. 185, 696 (1969).

52. B. B. Triplett, Ph.D. Thesis, University of California, Berkeley, UCRL-19672, Sept. 1970.

53. N. M. Senozan, Ph.D. Thesis, University of California, Berkeley, UCRL-11901, Jan. 1965.

54. Magnion Inc., Burlington, Mass.

55. Stycast 2850 GT, supplied by Emerson and Cuming Inc., Gardena, Calif.

56. J. E. Neighbor, Rev. Sci. Instr. 37, 497 (1966).

57. CryoCal Inc., Riviera Beach, Fla.

58. Apiezon T. grease, made by Associated Electrical Industries Ltd. (England), supplied by Shell Co.

59. Cominco Products Inc., Spokane, Wash.

60. E. F. Westrum Jr., C. Chou, D. W. Osborne, and H. E. Flotow, Cryogenics 7, 43 (1967).

61. H. Plumb and G. Cataland, Metrologia 2, 18 (1966).

62. H. van Dijk, M. Durieux, J. R. Clement, and J. K. Logan, J. Res. Natl. Bur. Std. (U.S.) 64A, 4 (1960).

63. R. B. Scott, G. A. Kilgore, and R. E. Gaumer, Natl. Bur. Std (U.S.) Progress Report 2 for Low Temp. Res., 21 (1948).

64. R. H.Sherman, S. G. Sydoriak, and T. R. Roberts, J. Res. Natl. Bur. Std. (U.S.) 68A, 579 (1964).

65. 2 model 145 fused quartz Bourdon tube Precision Pressure Gages from Texas Instruments Inc., Houston, Texas. One measures 0-300 torr, the other 0-1000 torr.

66. R. A. Watkins, W. L. Taylor, and W. S. Haubach, J. Chem. Phys. 46, 1007 (1967).

67. S. G. Sydoriak and R. H. Sherman, J. Res. Natl. Bur. Std. (U.S.) 68A, 547 (1964).

68. W. H. Keesom, Helium (Elsevier, N.Y., 1942), p. 49.

69. The acoustically derived values of M. E. Boyd, S. Y. Larsen, and H. Plumb, J. Res. Natl. Bur. Std. (U.S.) 72A, 155 (1968) disagree significantly with those of Keesom, but only 4 are given for the 4 to 20 K range.

70. W. E. Keller, Phys. Rev. 97, 1 (1955).

71. J. E. Kilpatrick, W. E. Keller, and E. F. Hammel, Phys. Rev. 97, 9 (1955).

72. T. C. Cetas and C. A. Swenson, Phys. Rev. Letters 25, 338 (1970).

73. J. S. Rogers, R. J. Tainsh, M. S. Anderson, and C. A. Swenson, Metrologia 4, 47 (1968).

74. G. Cataland and H. Plumb, J. Res. Natl. Bur. Std. (U.S.) 69A, 531 (1965).

75. D. W. Osborne, H. E. Flotow, and F. Schreiner, Rev. Sci. Instr. 38, 159 (1967).

76. D. L. Martin, Rev. Sci. Instr. 38, 1738 (1967) and N. Waterhouse, Can. J. Phys. 47, 1485 (1969).

77. J. C. Holste, T. C. Cetas, and C. A. Swenson, to be published.

78. Minneapolis-Honeywell Regulator Co., Philadelphia, Penn.

79. Lunex Company, Pleasant Valley, Iowa.

80. Research Chemicals, Division of Nuclear Corporation of America, Phoenix, Arizona.

81. Obtained through United Mineral and Chemical Corporation, New York City, the United States distributor.

82. N. T. Panousis and K. A. Gschneidner, Jr., Solid State Comm. 8, 1779 (1970).

83. D. H. Parkinson and L. M. Roberts, Proc. Phys. Soc. B70, 471 (1957).

84. O. V. Lounasmaa, Phys. Rev. 133, A502 (1964).

85. M. Rosen, Phys. Rev. Letters 19, 695 (1967).

86. O. V. Lounasmaa and L. J. Sundström, Phys. Rev. 150, 399 (1966).

87. O. V. Lounasmaa, Phys. Rev. 133, A211 (1964).

88. O. V. Lounasmaa, Phys. Rev. 129, 2460 (1963).

89. O. V. Lounasmaa and P. R. Roach, Phys. Rev. 128, 622 (1962).

90. O. V. Lounasmaa and R. A. Guenther, Phys. Rev. 126, 1357 (1962).

91. N. E. Phillips, Crit. Rev. Solid State Sci. 2, 467 (1971).

92. F. Heiniger, E. Bucher, and M. Juller, Phys. kondens. Materie 5, 243 (1966).

93. J. F. Wilkins, J. G. Clark, and T. E. Leinhardt, Bull. Am. Phys. Soc. 7, 579 (1962).

94. H. V. Culbert, Phys. Rev. 156, 701 (1967).

95. S. Arajs and R. V. Colvin, J. Less-Common Metals 4, 159 (1962).

96. M. Rosen, Phys. Rev. 180, 540 (1969).

97. G. S. Fleming and T. L. Loucks, Phys. Rev. 173, 685 (1968).

98. W. C. Koehler, J. Appl. Phys. 36, 1078 (1965).

99. J. A. Morrison and D. M. T. Newsham, J. Phys. C 1, 370 (1968).

100. D. L. Johnson and D. K. Finnemore, Phys. Rev. 158, 376 (1967).

101. B. Dreyfus, J. C. Michel, D. Thoulouze, Phys. Letters 24A, 457 (1967).

102. R. D. Parks, Proc. IInd Conf. Rare Earth Research, J. F. Nachman and C. E. Lundin, eds., (Gordon and Breach, N.J., 1962), p. 225.

103. Recalculated by the author.

104. L. M. Roberts and J. M. Lock, Phil. Mag. 2, 811 (1957).

105. S. Arajs and G. R. Dunmyre, J. Less-Common Metals 12, 162 (1967).

Figure Captions

1. Phase diagram of Ce. The α-α' phase boundary has not been studied above 480 K.
2. Calorimeter used for measurements on Ce between 0.4 and 24 K.
3. The low temperature heat capacity of LU Ce.
4. The intermediate temperature heat capacity of LU Ce.
5. The high temperature heat capacity of LU Ce.
6. The heat capacity of RC Ce. Less than half the points below 4 K are shown. The smooth curve representing the heat capacity of LU Ce is drawn through points shown in figures 3-5.
7. The heat capacity of JMA Ce. Less than half the points below 4 K are shown. The smooth curve representing the heat capacity of LU Ce is drawn through points shown in figures 3-5.
8. The heat capacity of JMB Ce. Less than half the points below 4 K are shown. The smooth curve representing the heat capacity of LU Ce is drawn through points shown in figures 3-5.
9. The heat capacity of PGβ Ce. Less than half the points below 4 K are shown. The smooth curve representing the heat capacity of LU Ce is drawn through points shown in figures 3-5.
10. The heat capacity of PGα Ce. Less than half the points below 4 K are shown. The smooth curve representing the heat capacity of LU Ce is drawn through points shown in figures 3-5.
11. The heat capacity of PR Ce. Less than half the points below 4 K are shown. The smooth curve representing the heat capacity of LU Ce is drawn through points shown in figures 3-5.

12. The low temperature heat capacity and the extrapolation of γ_o of RC Ce.
13. The low temperature heat capacity and the extrapolation of γ_o of JMA Ce.
14. The low temperature heat capacity and the extrapolation of γ_o of JMB Ce.
15. The low temperature heat capacity and the extrapolation of γ_o of LO Ce.
16. A typical low temperature heat capacity and extrapolation of γ_o of LU Ce.
17. The heat capacity of heavily oxidized LU Ce. Less than half the points below 4 K are shown. The smooth curve representing the heat capacity of unoxidized LU Ce is drawn through points shown in figures 3-5.
18. The effect of a 60.5 kOe field on the heat capacity of RC Ce. The smooth curve representing the zero field heat capacity of RC Ce is drawn through the points shown in figure 6.
19. The 0.15 K peaks and hyperfine heat capacities of LU and RC Ce.
20. The 0.15 K peaks of RC and LU Ce.
21. The 0.9 K peak of LU Ce.
22. The 6 K peak of LU Ce.

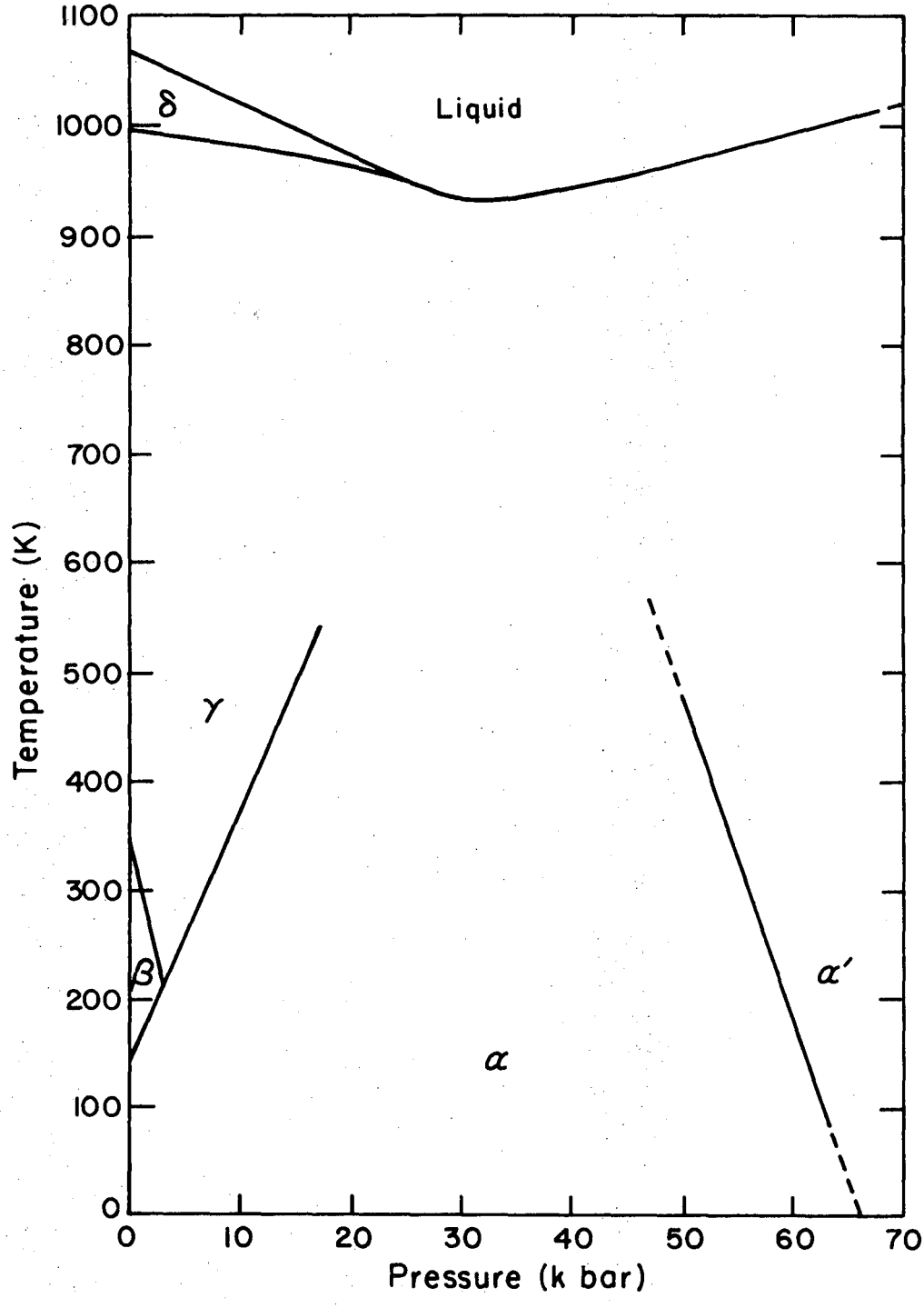
1100
1000
900
800
700
600
500
400
300
200
100
0
Temperature (K)
δ
Liquid
γ
β
α
α'
0
10
20
30
40
50
60
70
Pressure (k bar)
XBL725-6225

Figure 1

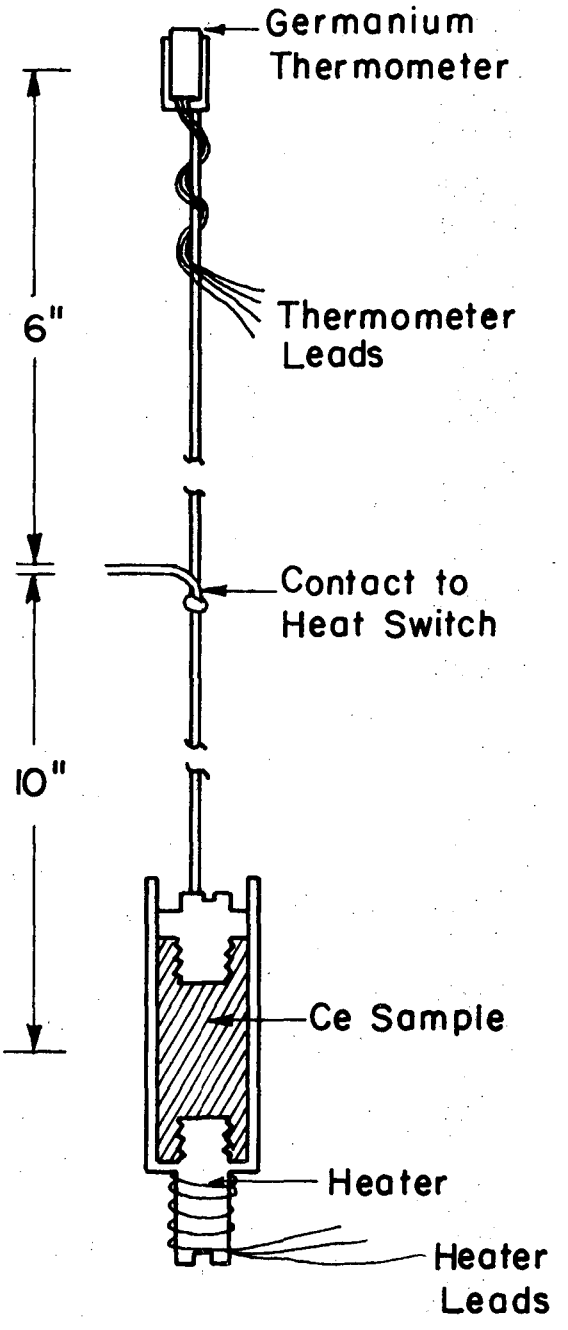

XBL 725 - 6226

Figure 2

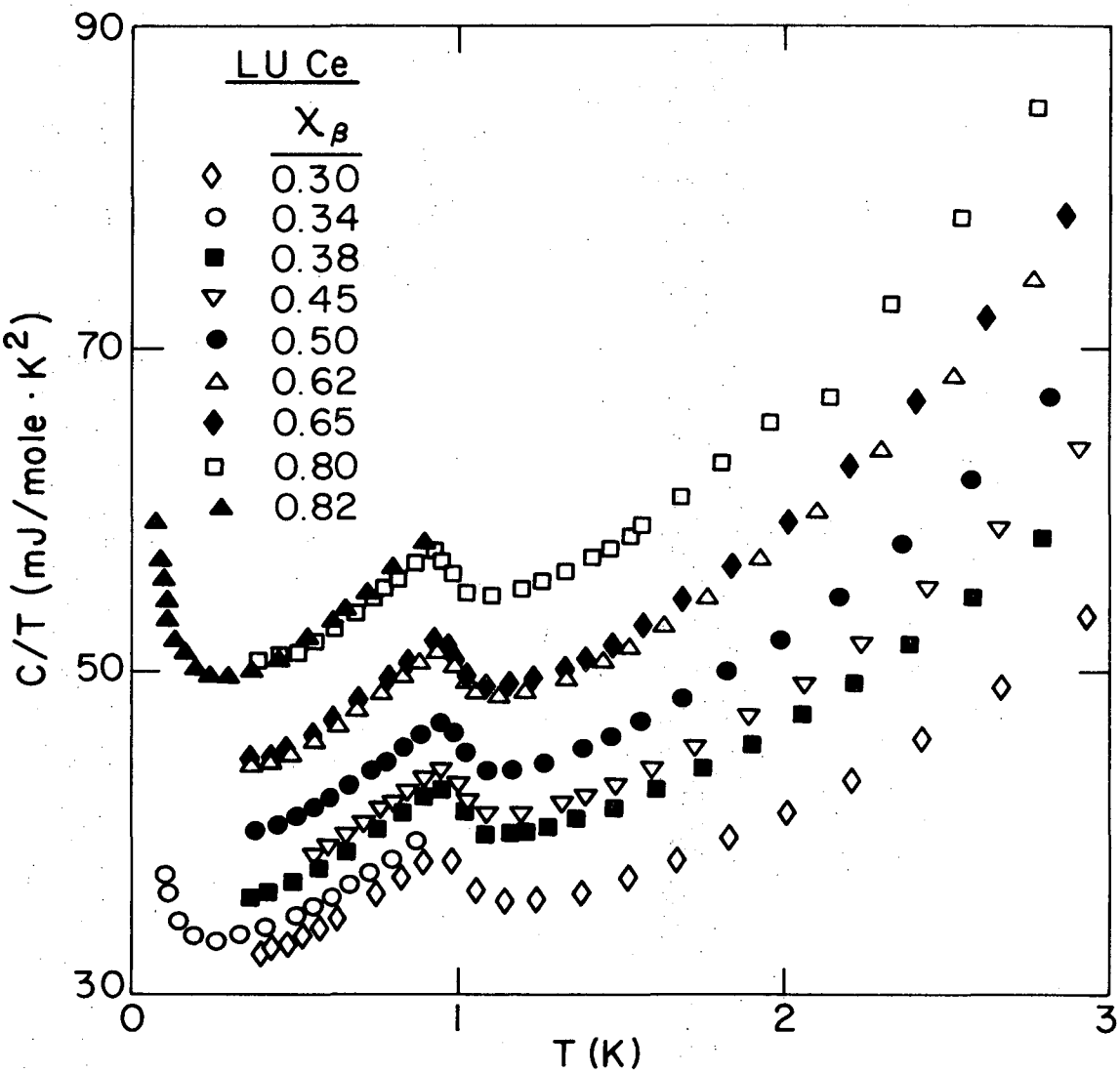
LU Ce
X_β
0.30
0.34
0.38
0.45
0.50
0.62
0.65
0.80
0.82
C/T (mJ/mole · K²)
T (K)
90
70
50
30
0
1
2
3
XBL 725-6227

Figure 3

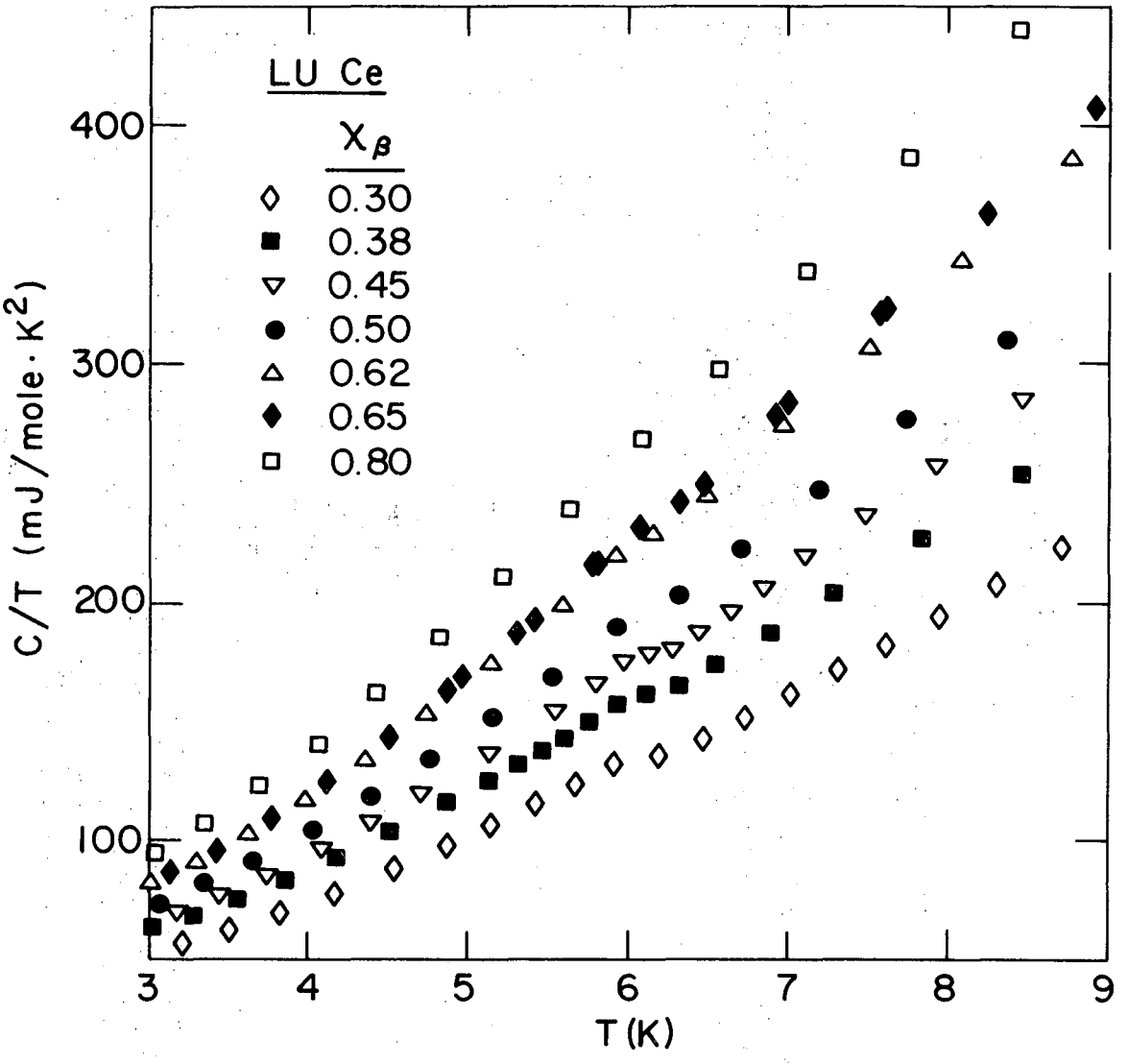

Figure 4

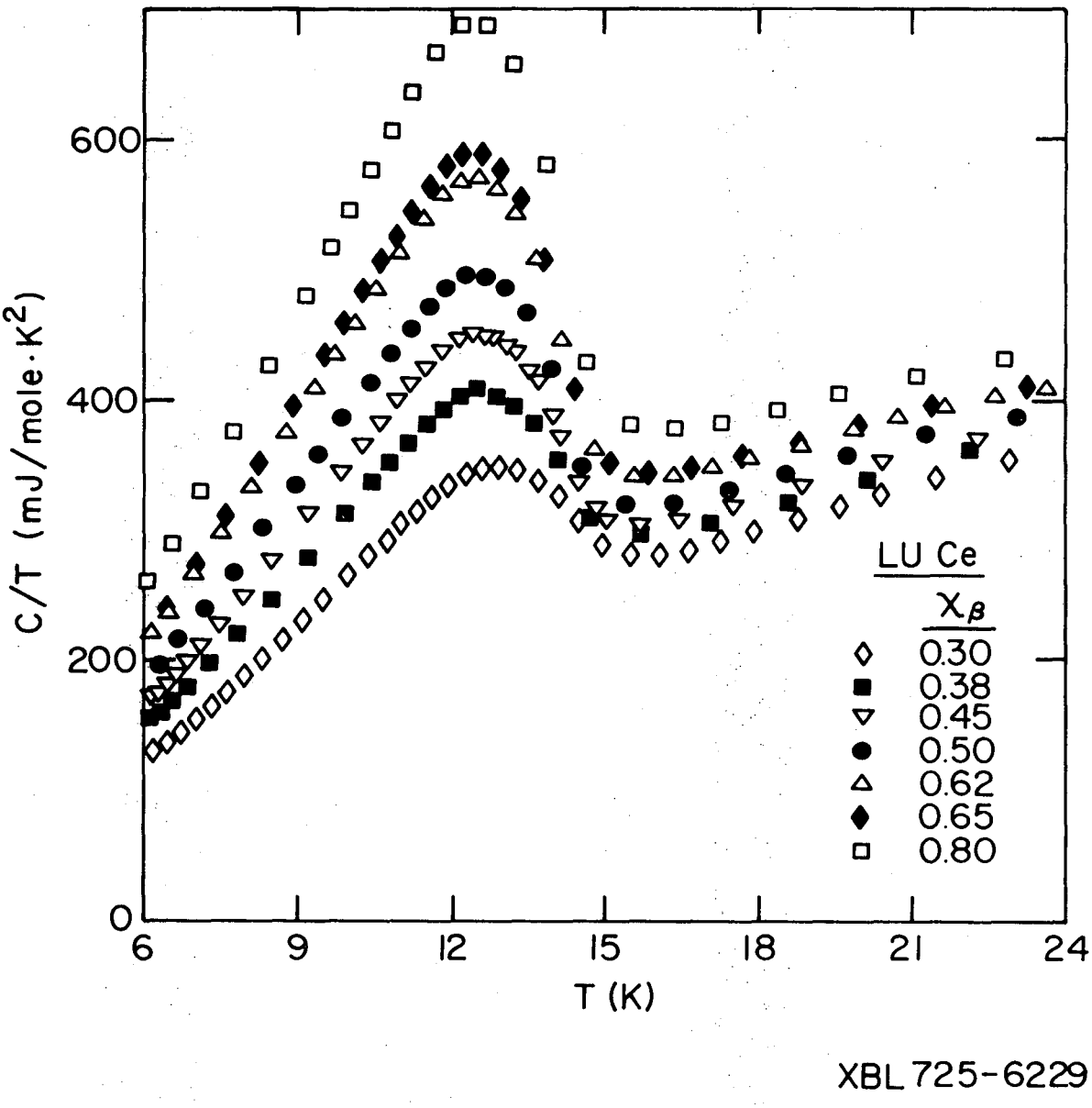
C/T (mJ/mole·K²)
600
400
200
0
6
9
12
15
18
21
24
T (K)
LU Ce
X_β
0.30
0.38
0.45
0.50
0.62
0.65
0.80
XBL 725-6229

Figure 5

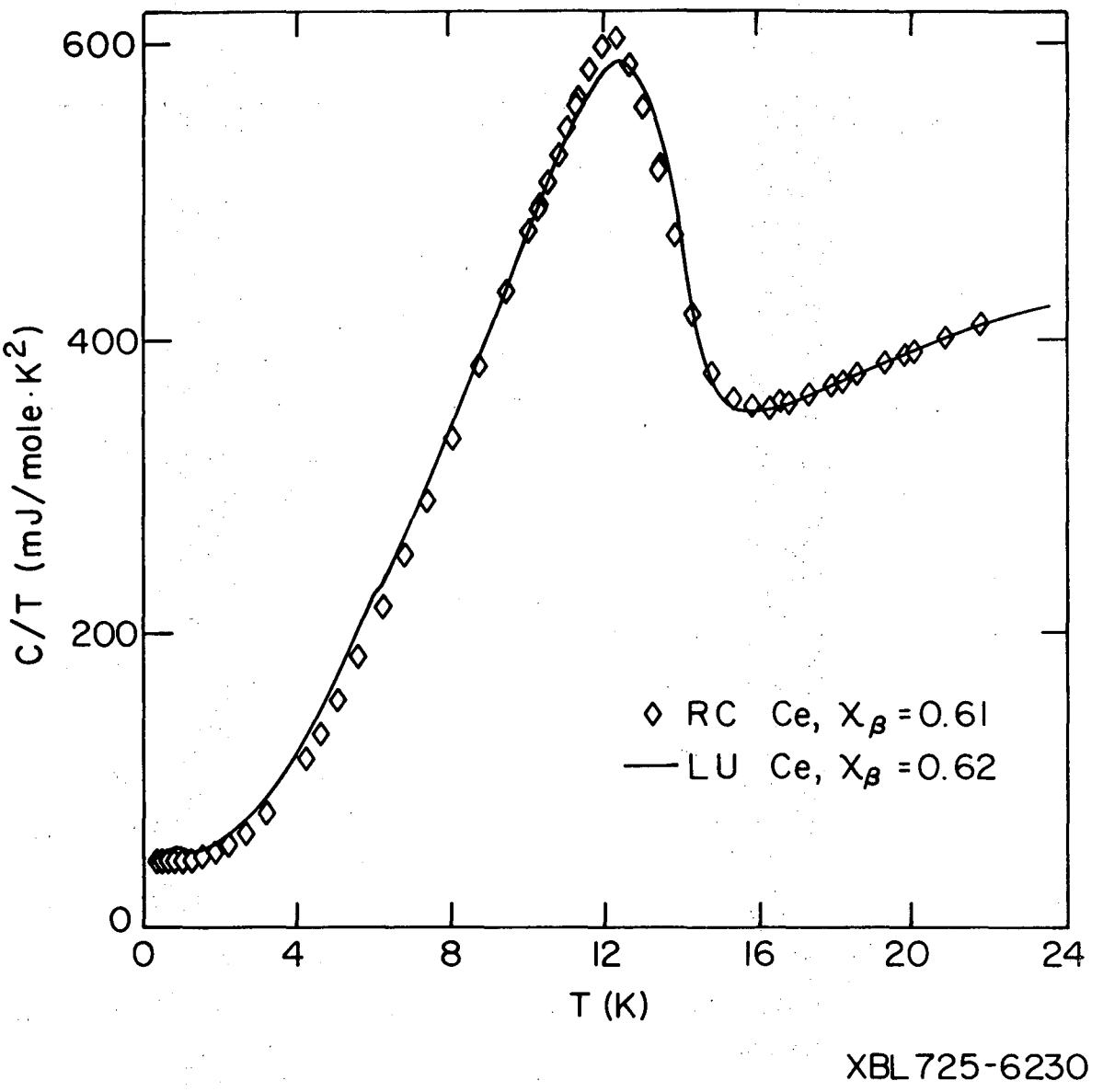
600
400
200
0
C/T (mJ/mole·K²)
0
4
8
12
16
20
24
T (K)
◇ RC Ce, X_β = 0.61
— LU Ce, X_β = 0.62
XBL725-6230

Figure 6

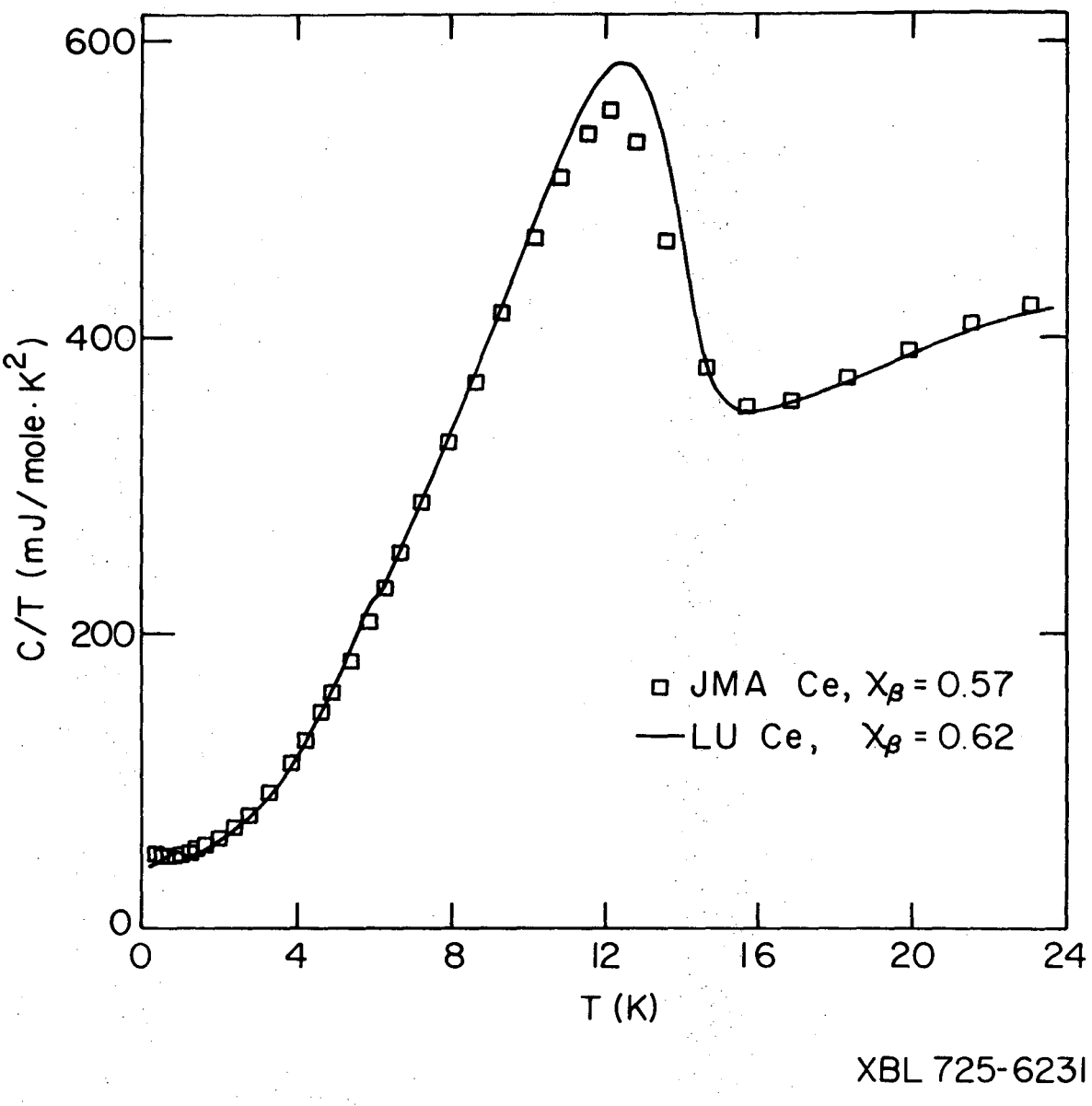
600
400
200
0
C/T (mJ/mole·K²)
0
4
8
12
16
20
24
T (K)
□ JMA Ce, X_β = 0.57
—LU Ce, X_β = 0.62
XBL 725-6231

Figure 7

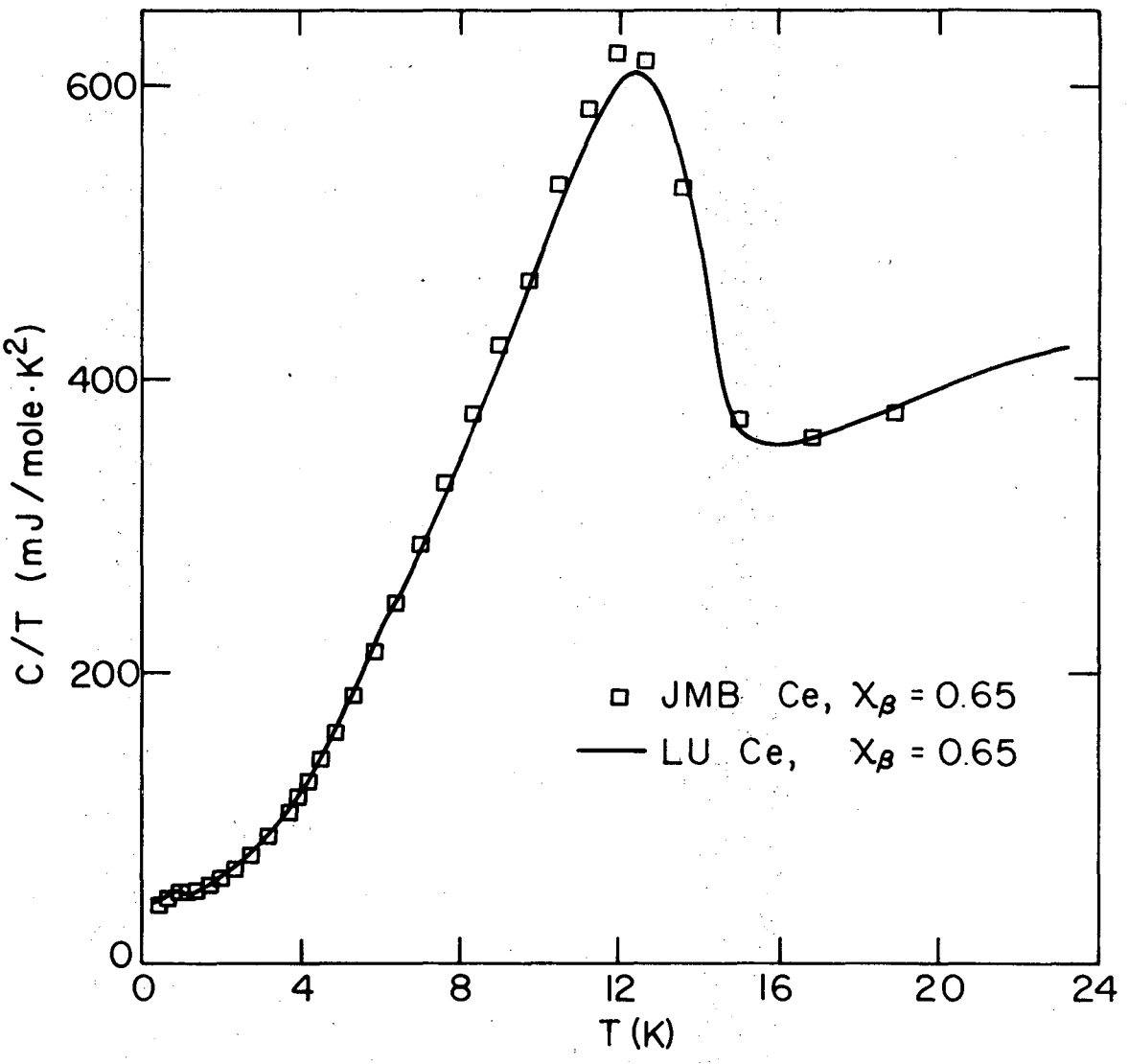

Figure 8

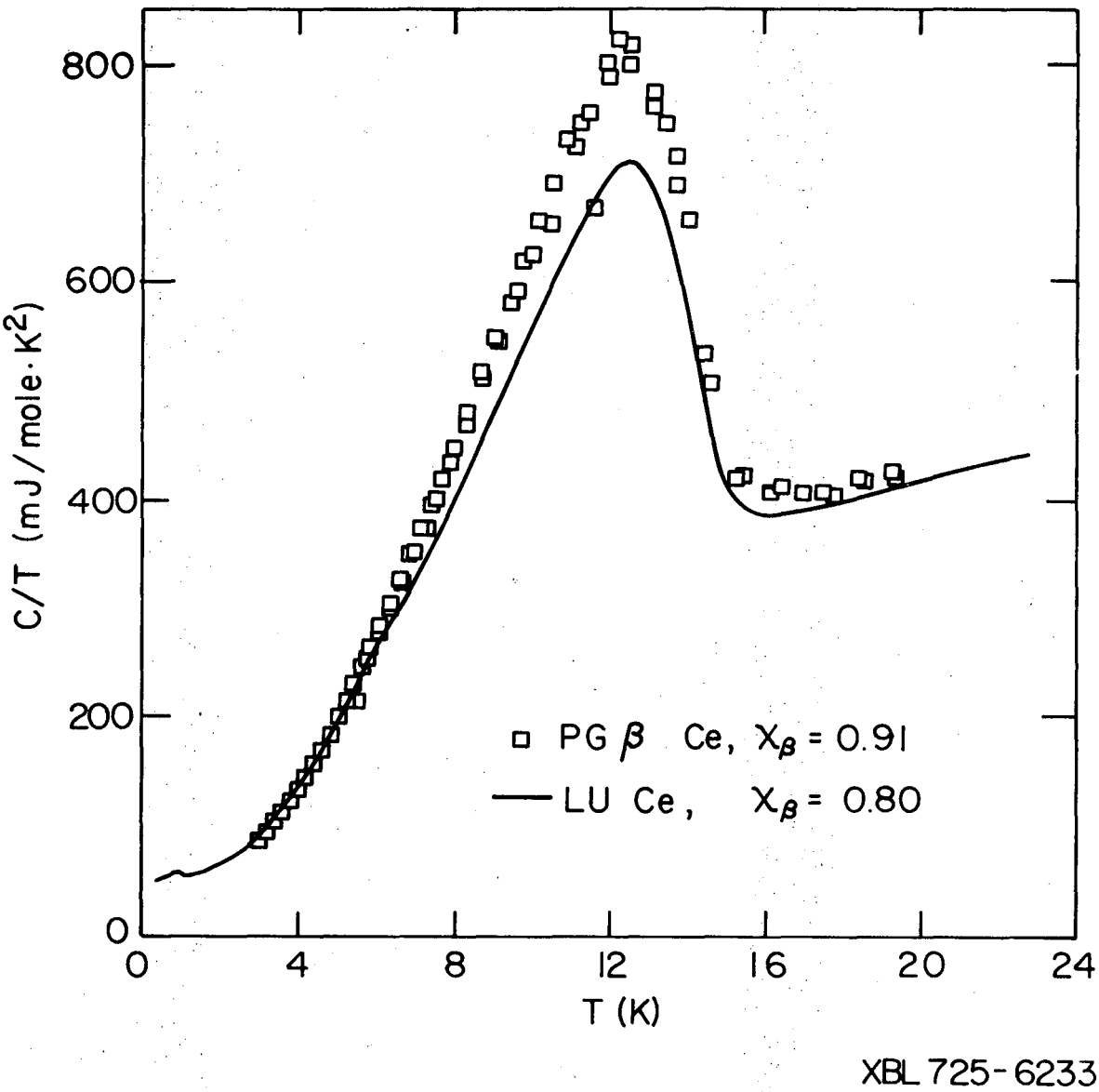
800
600
400
200
0
C/T (mJ/mole·K²)
0
4
8
12
16
20
24
T (K)
PG β Ce, X_β = 0.91
LU Ce, X_β = 0.80
XBL 725-6233

Figure 9

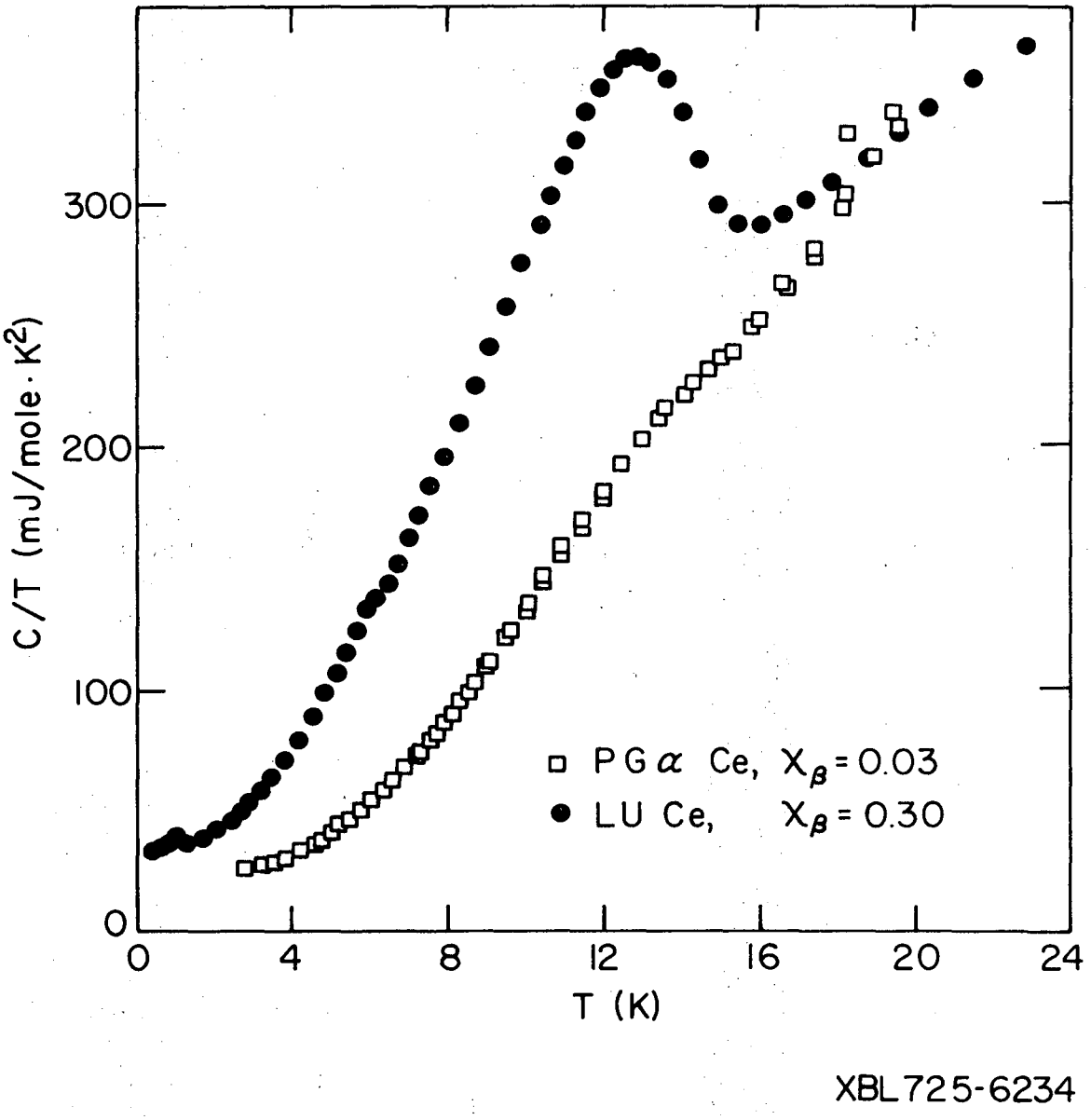
C/T (mJ/mole · K²)
300
200
100
0
0
4
8
12
16
20
24
T (K)
□ PG α Ce, $X_\beta = 0.03$
● LU Ce, $X_\beta = 0.30$
XBL725-6234

Figure 10

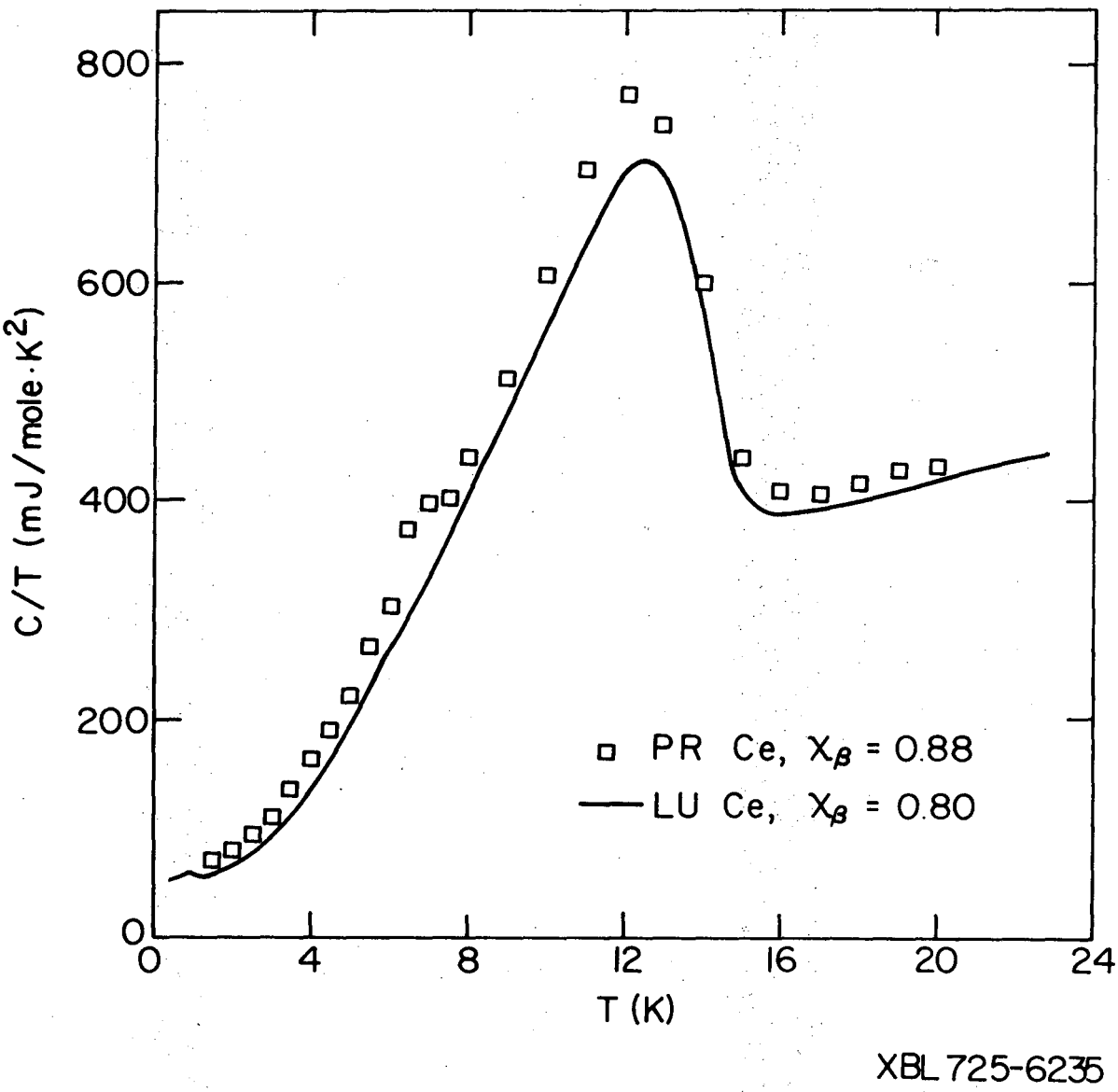
800
600
400
200
0
C/T (mJ/mole·K²)
0
4
8
12
16
20
24
T (K)
PR Ce, X_β = 0.88
LU Ce, X_β = 0.80
XBL 725-6235

Figure 11

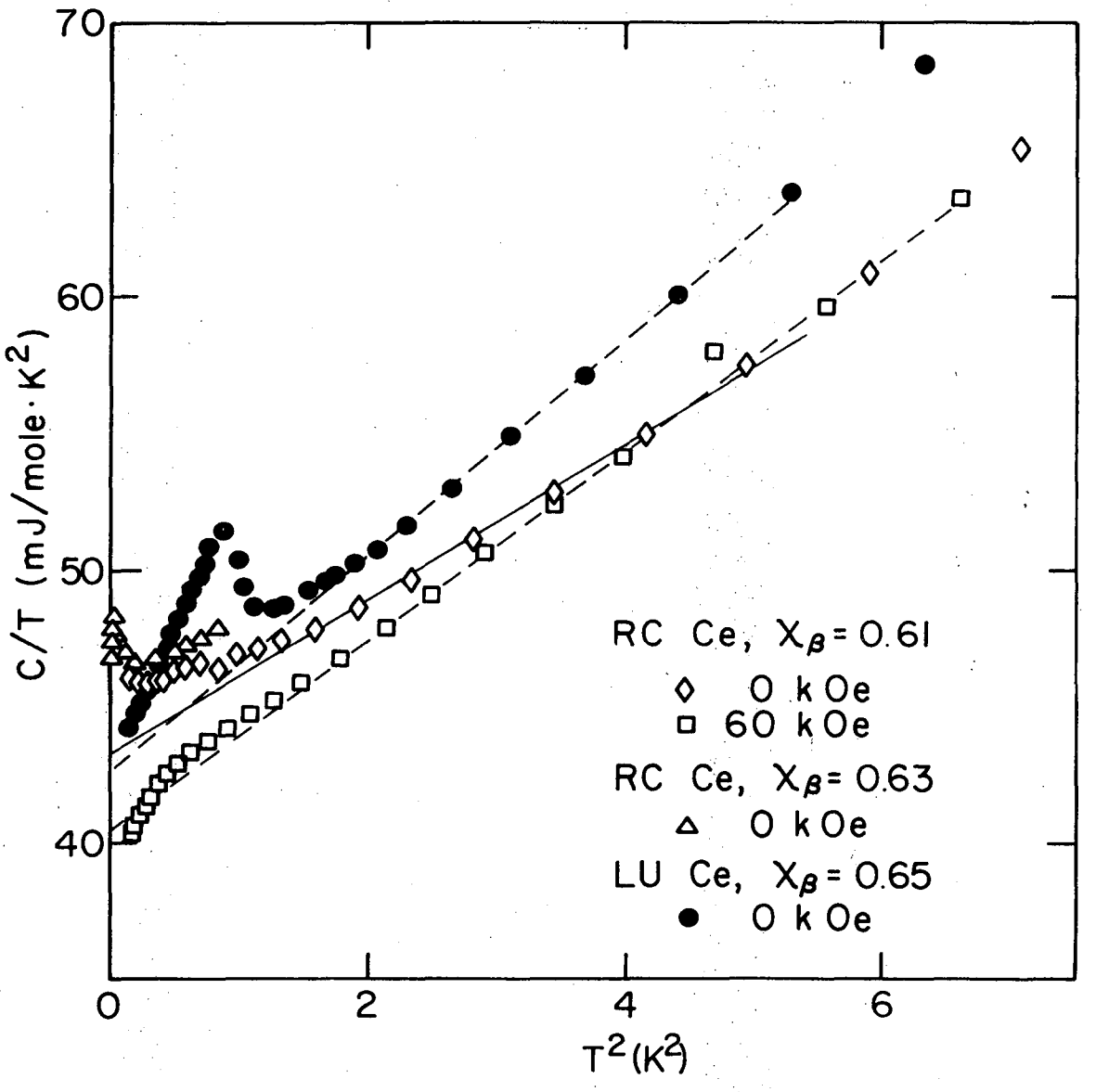

XBL 725-6236

Figure 12

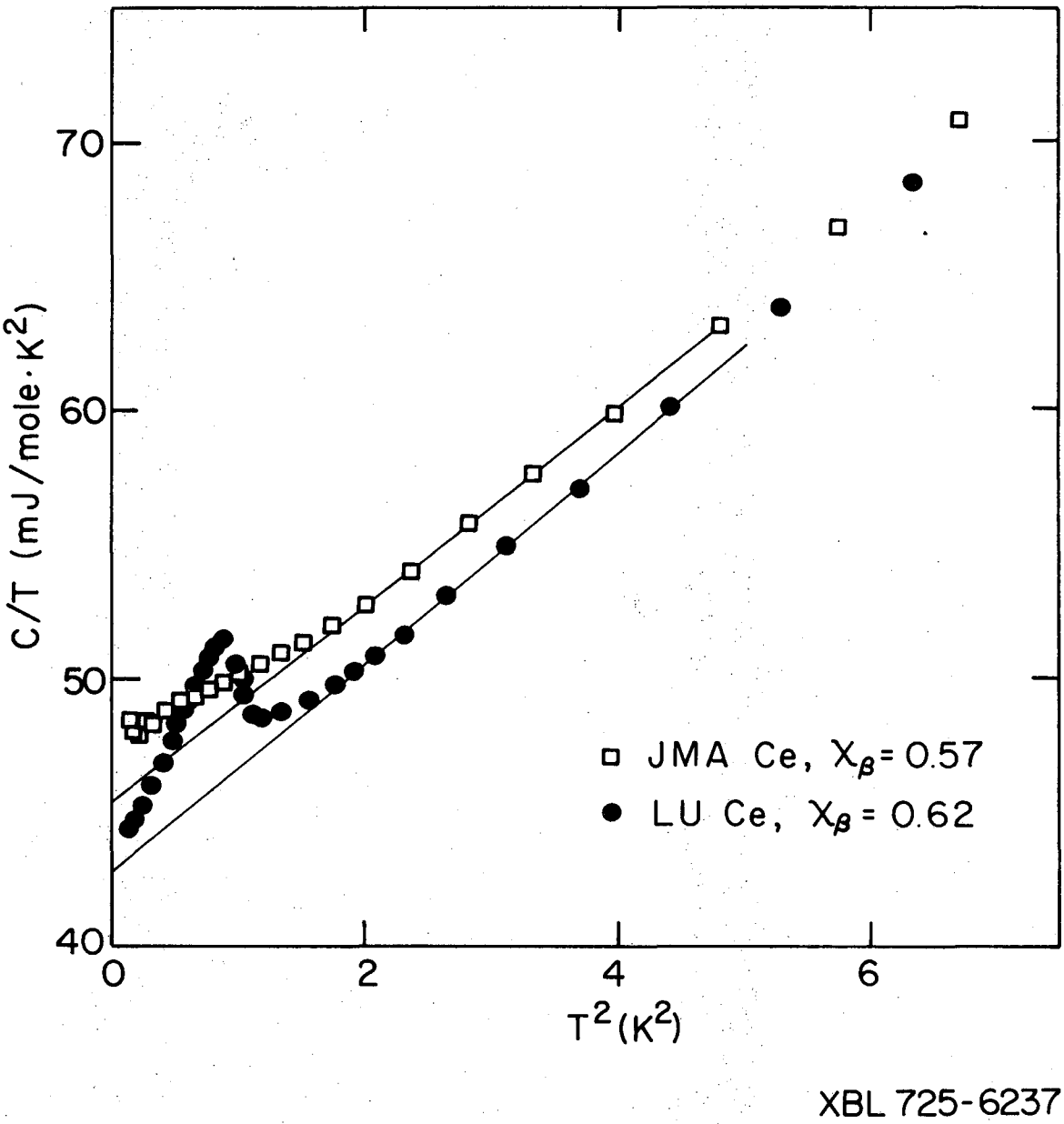
70
60
50
40
C/T (mJ/mole·K²)
0
2
4
6
T²(K²)
JMA Ce, Xβ = 0.57
LU Ce, Xβ = 0.62
XBL 725-6237

Figure 13

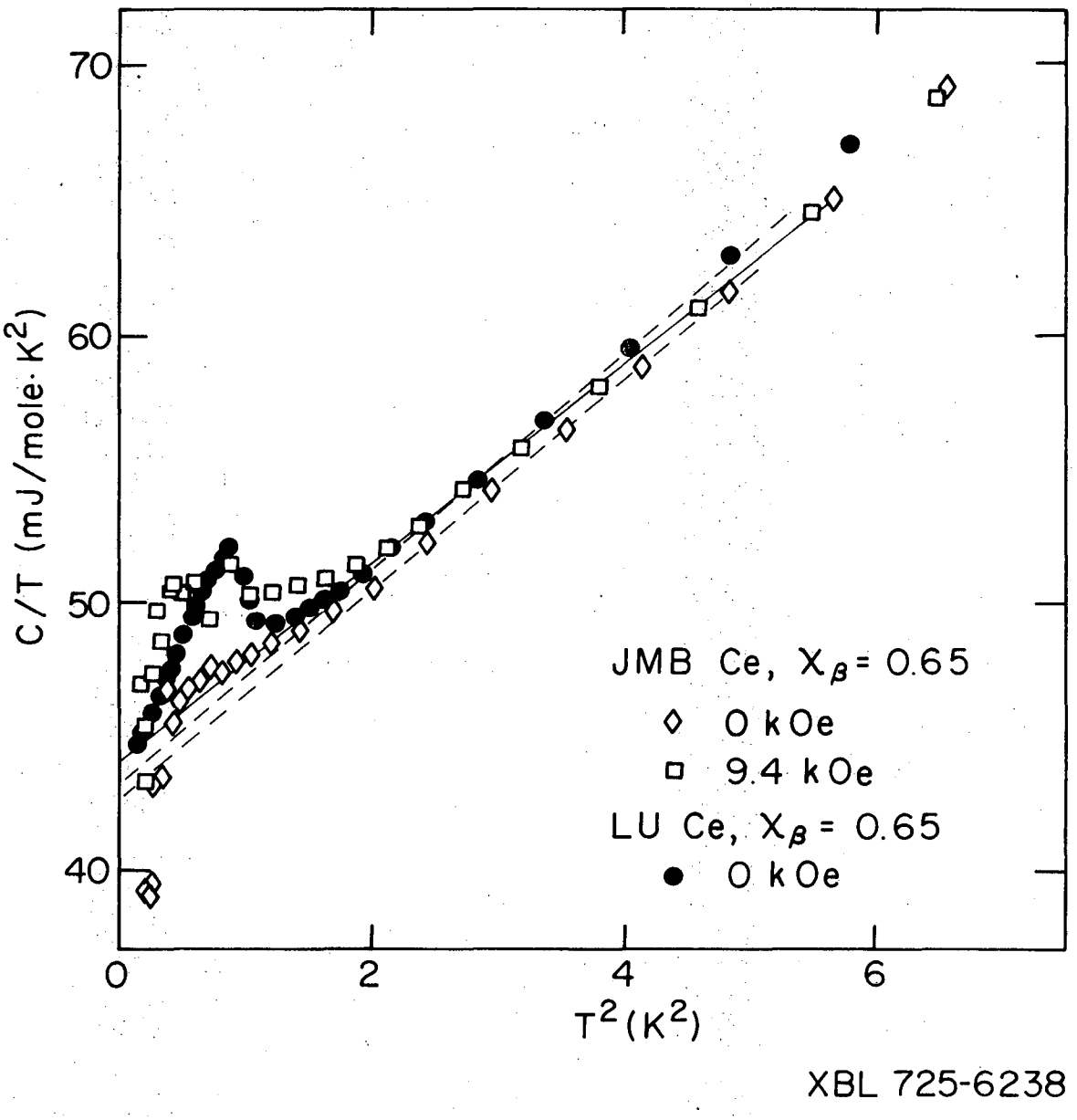

Figure 14

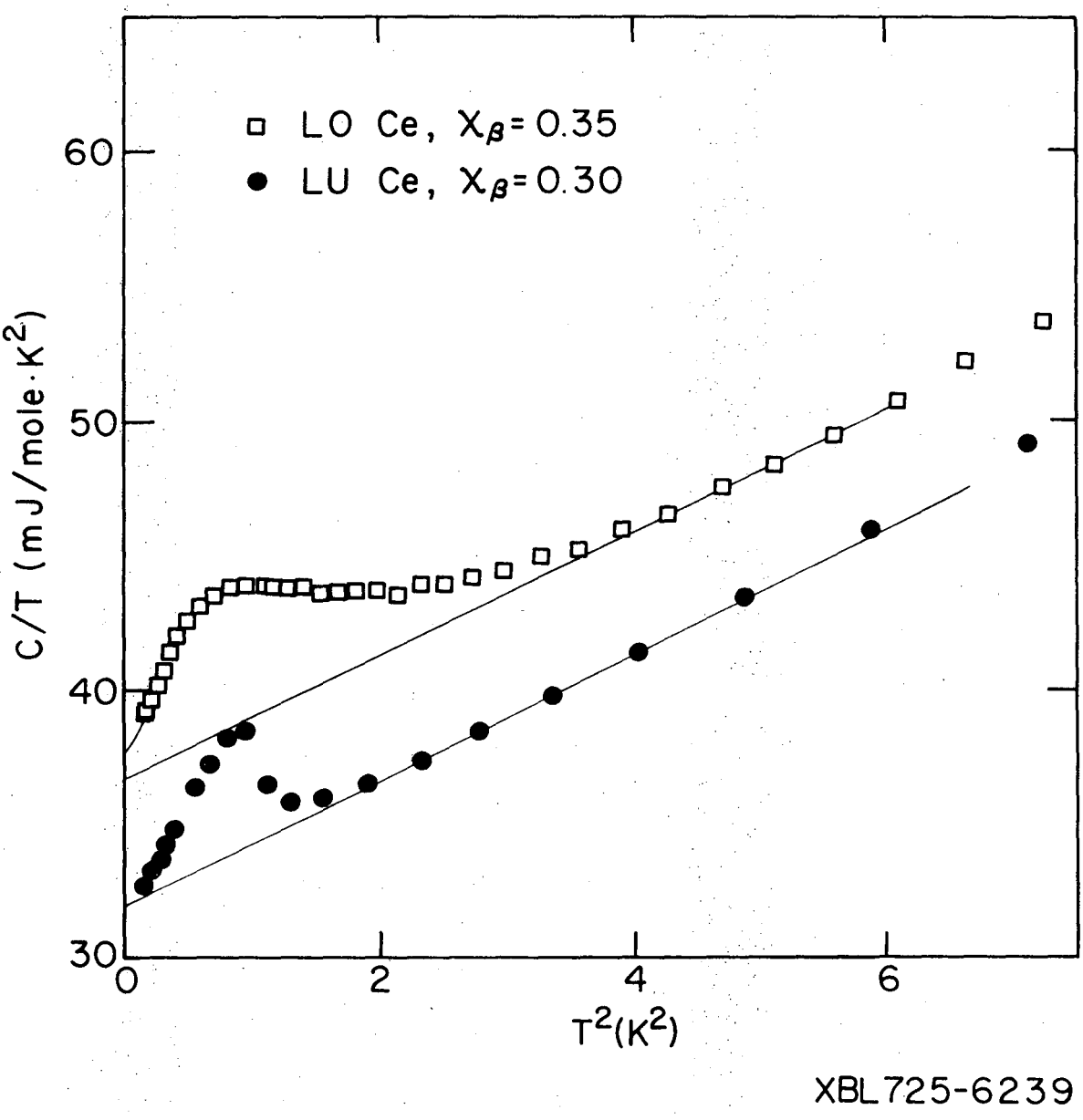
LO Ce, X_β= 0.35
LU Ce, X_β= 0.30
C/T (mJ/mole·K²)
60
50
40
30
0
2
4
6
T²(K²)
XBL725-6239

Figure 15

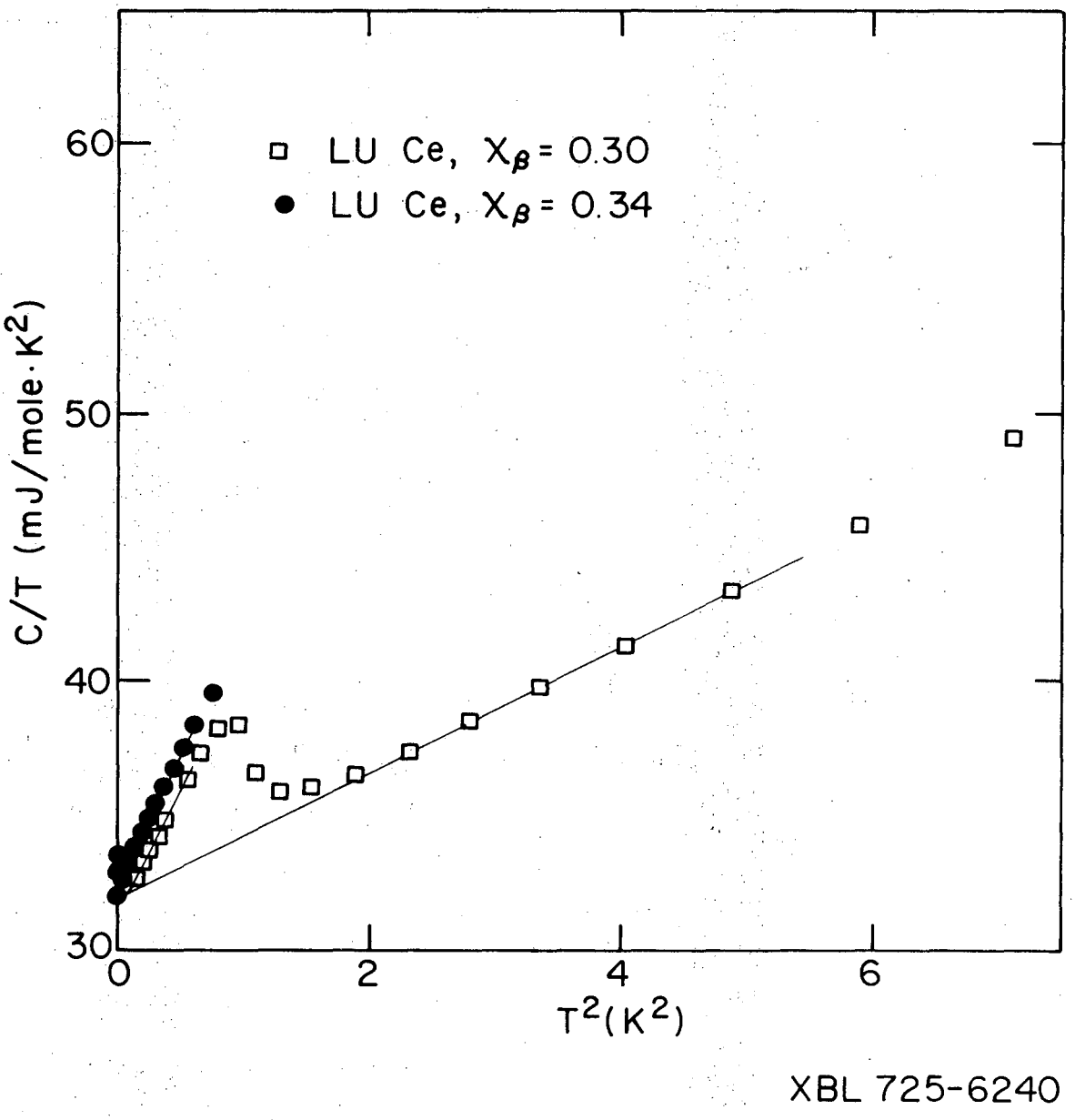

Figure 16

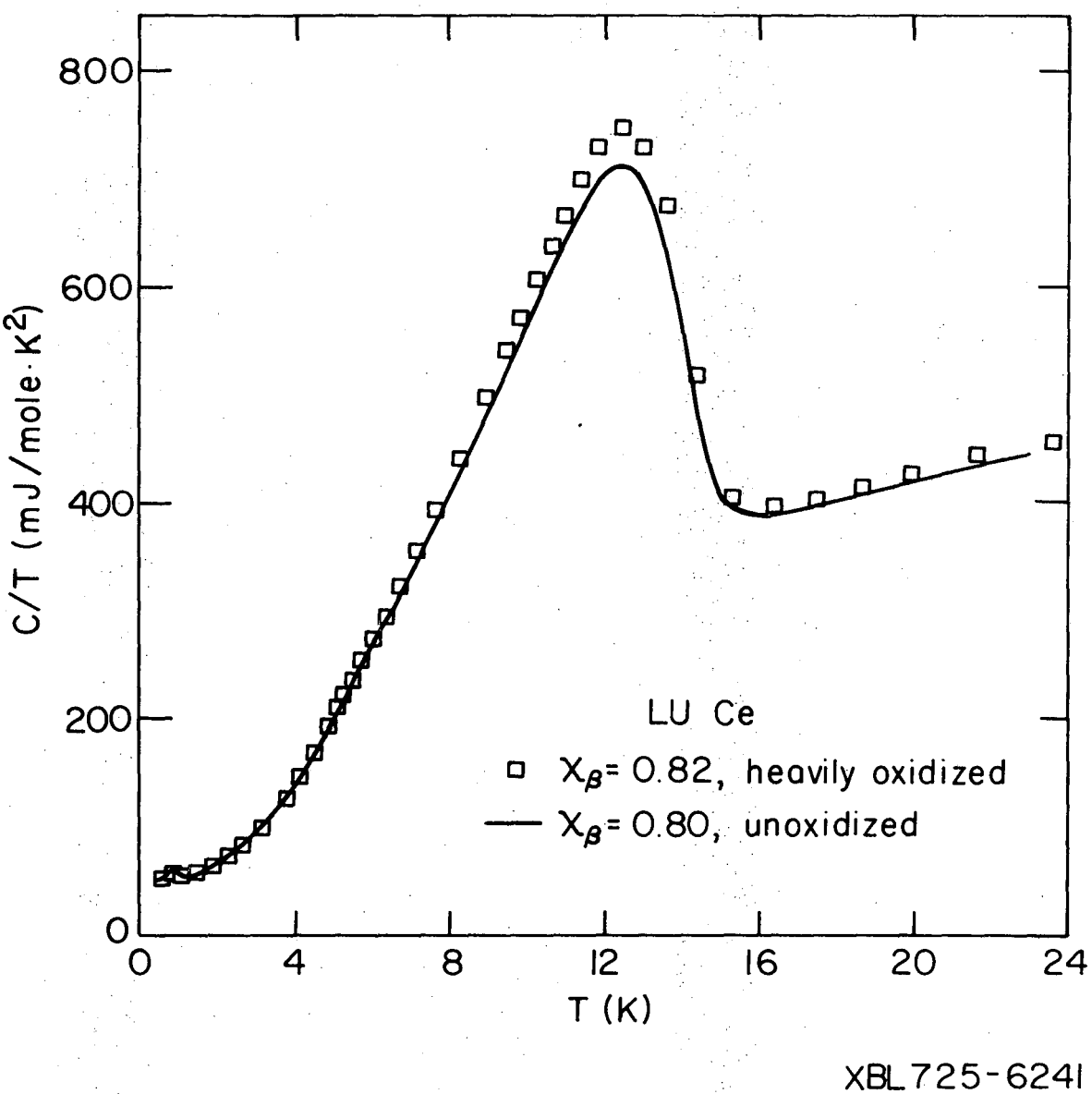
800
600
400
200
0
C/T (mJ/mole·K²)
0
4
8
12
16
20
24
T (K)
LU Ce
□ X_β= 0.82, heavily oxidized
— X_β= 0.80, unoxidized
XBL725-6241

Figure 17

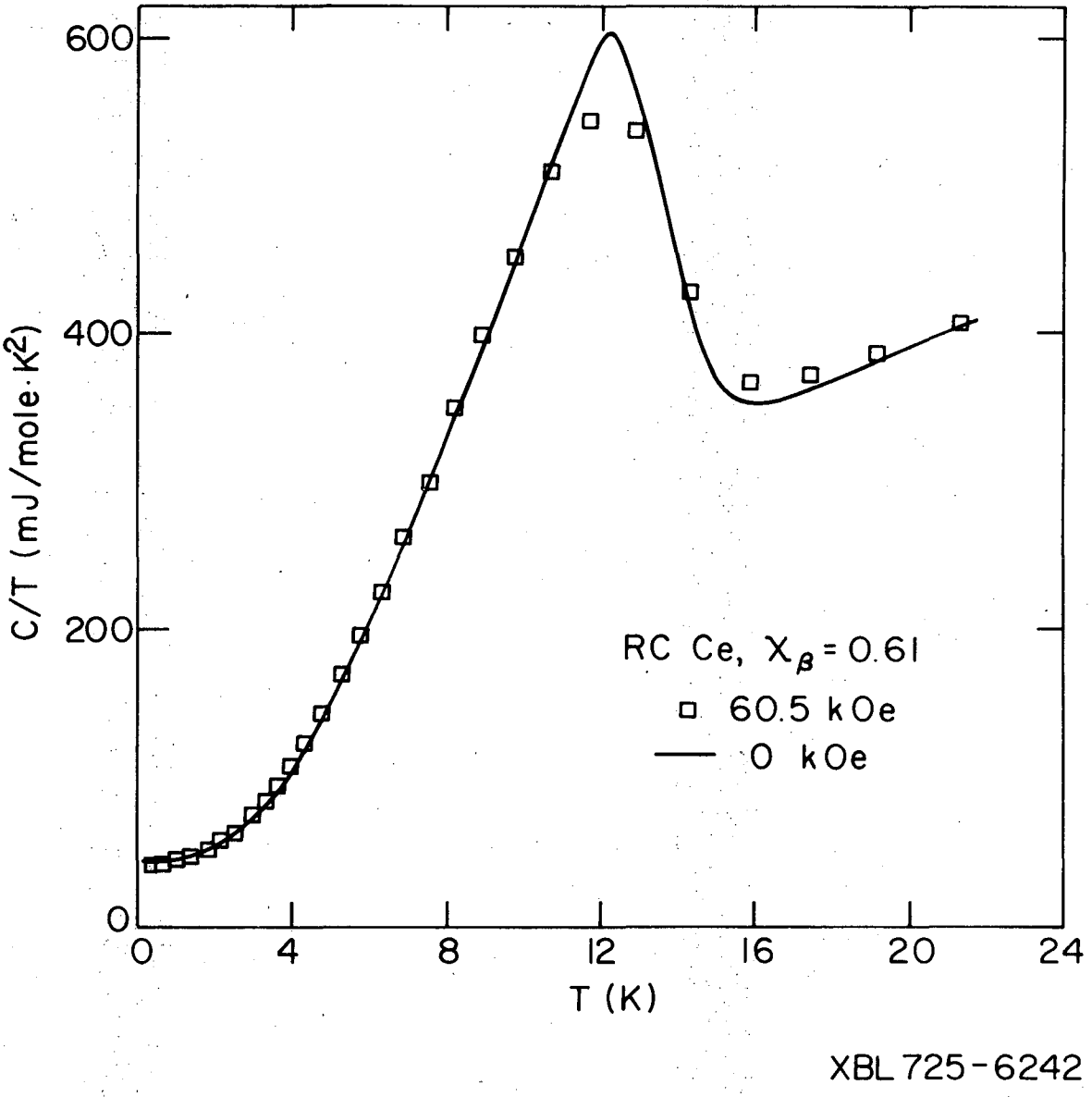
600
400
200
0
C/T (mJ/mole·K²)
0
4
8
12
16
20
24
T (K)
RC Ce, $X_\beta = 0.61$
60.5 kOe
0 kOe
XBL 725-6242

Figure 18

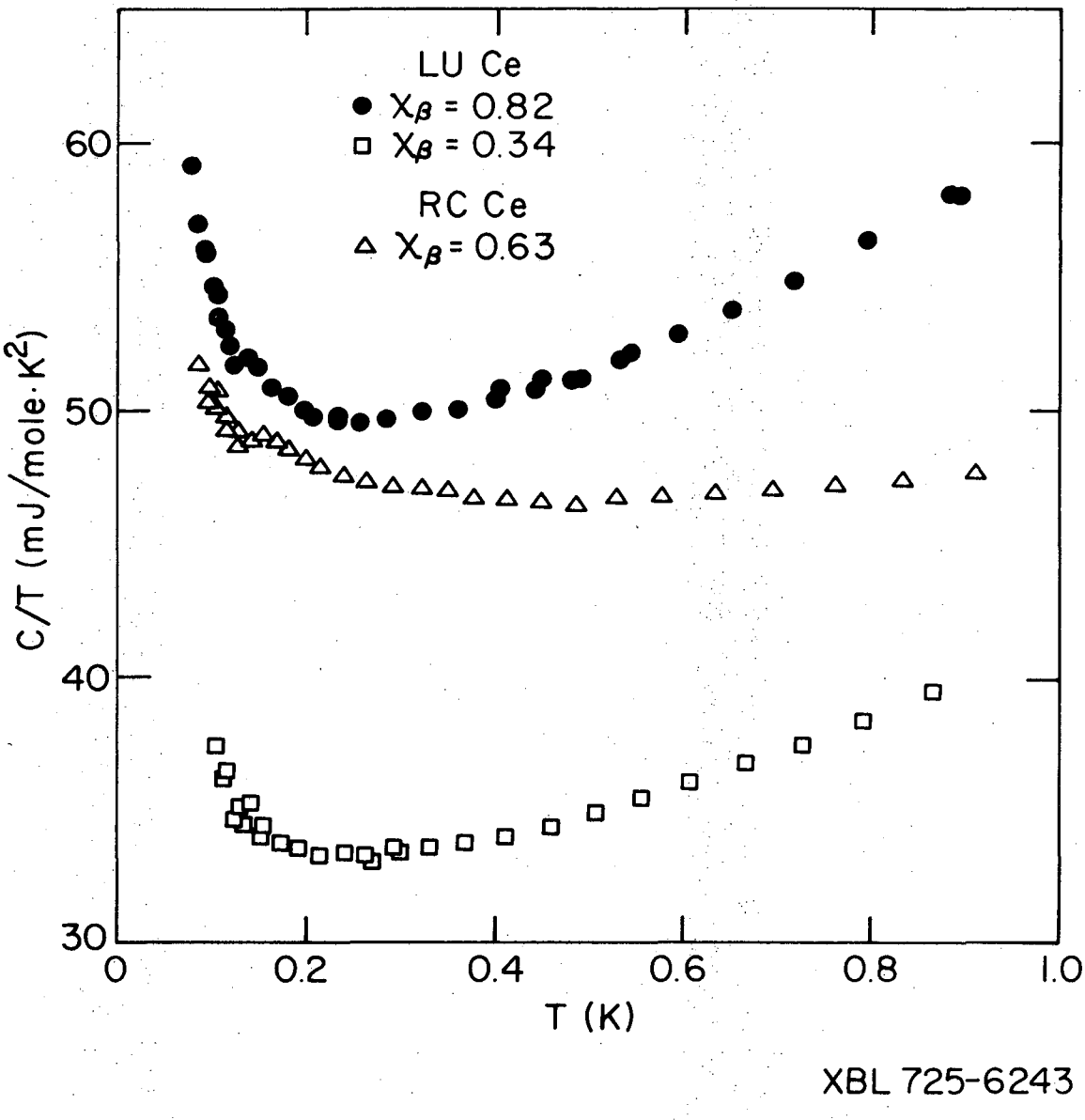
LU Ce
X_β = 0.82
X_β = 0.34
RC Ce
X_β = 0.63
C/T (mJ/mole·K²)
60
50
40
30
0
0.2
0.4
0.6
0.8
1.0
T (K)
XBL 725-6243

Figure 19

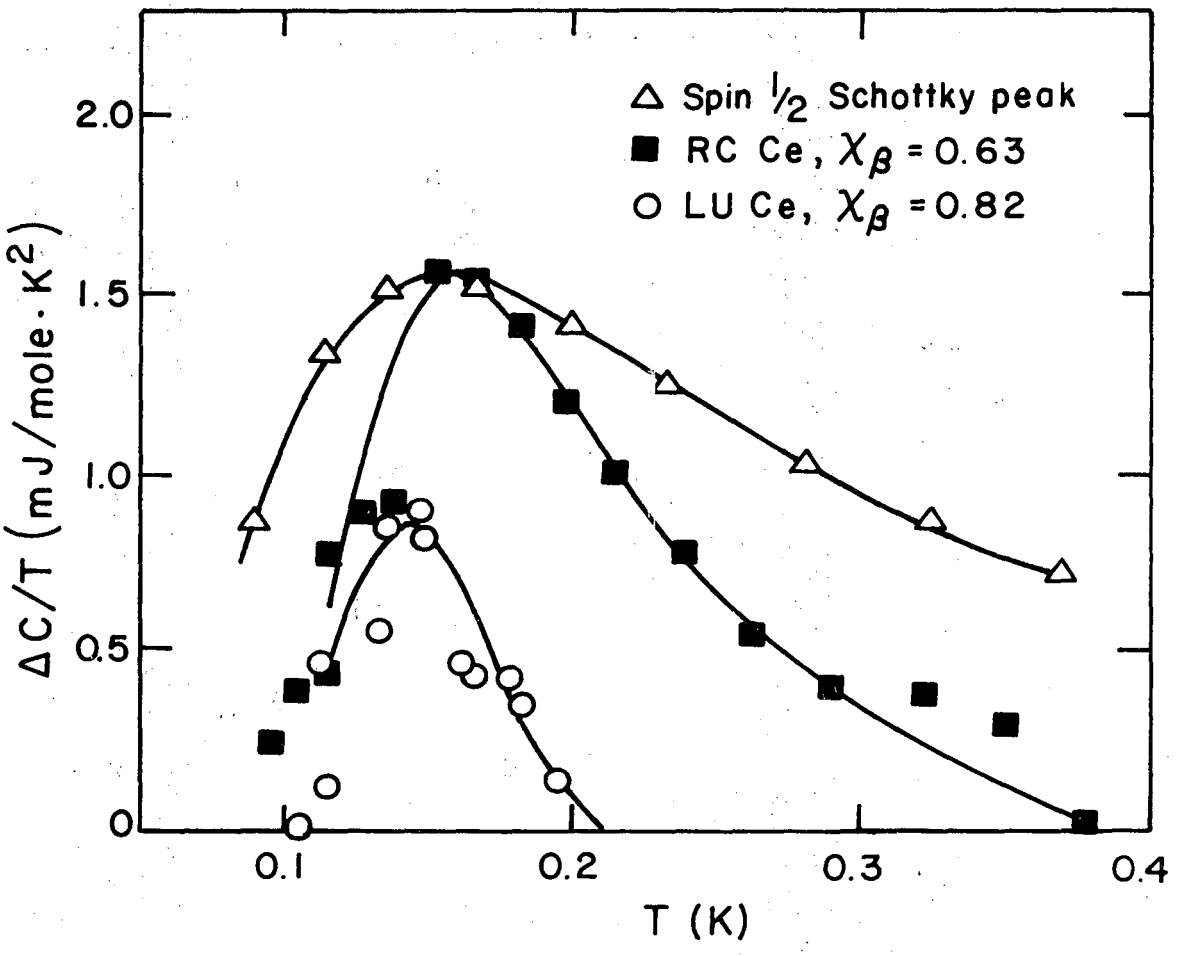
Δ Spin 1/2 Schottky peak
■ RC Ce, χ_β = 0.63
○ LU Ce, χ_β = 0.82
ΔC/T (mJ/mole·K²)
2.0
1.5
1.0
0.5
0
0.1
0.2
0.3
0.4
T (K)
XBL725-6244

Figure 20

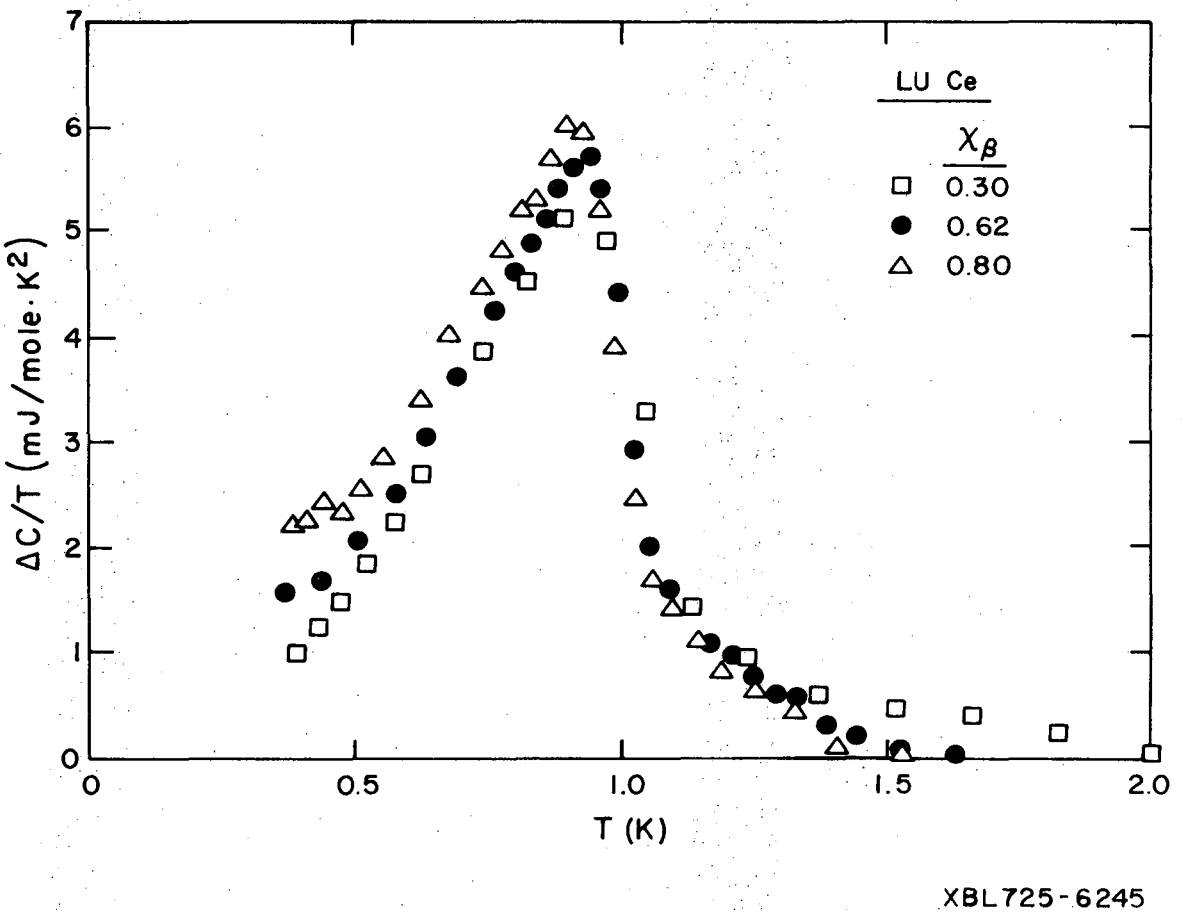
LU Ce
χ_β
0.30
0.62
0.80
ΔC/T (mJ/mole·K²)
T (K)
0
0.5
1.0
1.5
2.0
1
2
3
4
5
6
7
XBL725-6245

Figure 21

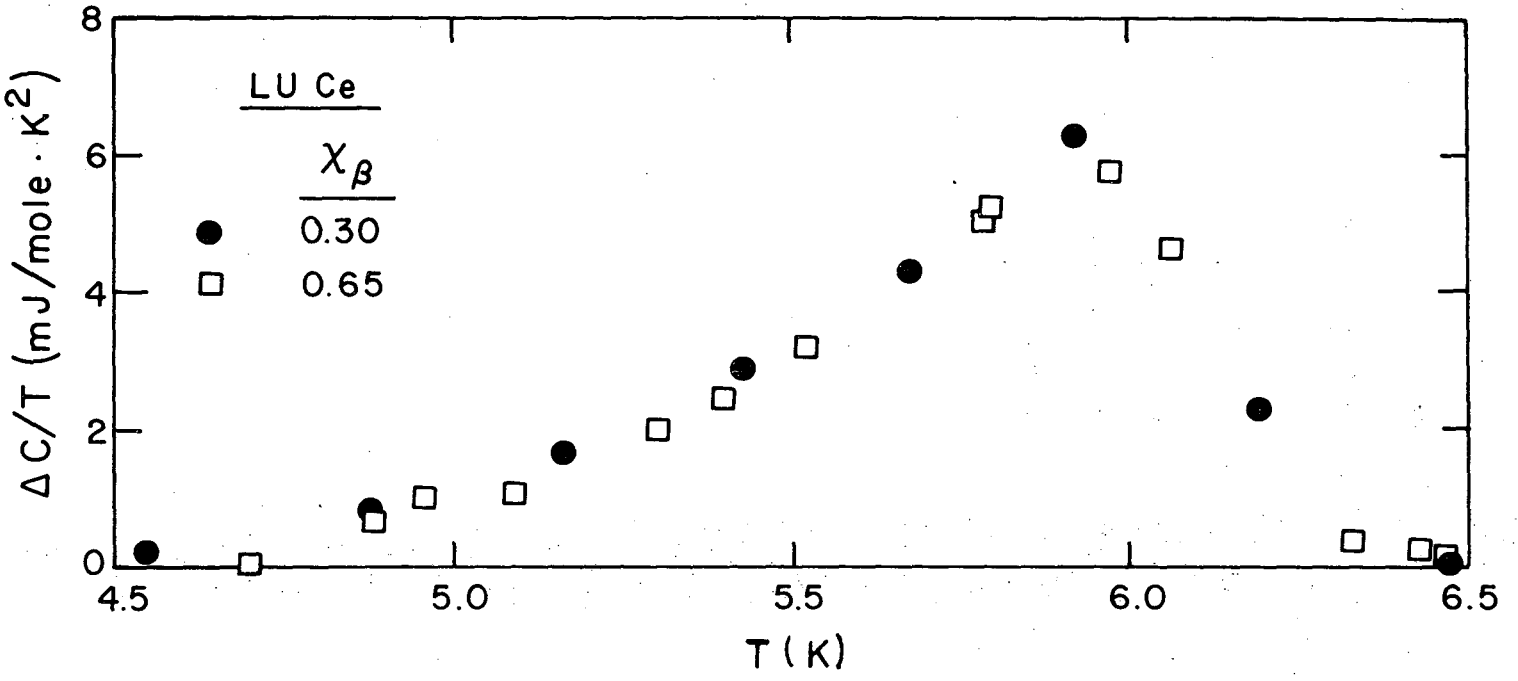

XBL725-6246

Figure 22

Acknowledgments

I would like to thank Dr. N. E. Phillips for suggesting this project and for his helpful discussions and advice, and thank also the other members of this research group for the times when they were helpful and informative.

The calorimeter used in the 0.08 to 8 K measurements was designed and calibrated by B. B. Triplett.

This work was performed under the auspices of the U. S. Atomic Energy Commission. I also received a National Science Foundation fellowship for 2 years.

TECHNICAL INFORMATION DIVISION
LAWRENCE BERKELEY LABORATORY
UNIVERSITY OF CALIFORNIA
BERKELEY, CALIFORNIA 94720